

TECHNICAL UNIVERSITY OF LIBEREC



FACULTY OF TEXTILE ENGINEERING

DIPLOMA THESIS

Liberec 2013

Funda Büyük Mazari

TECHNICAL UNIVERSITY OF LIBEREC
FACULTY OF TEXTILE ENGINEERING

DIPLOMA THESIS

Liberec 2013

Funda Büyük Mazari

TECHNICAL UNIVERSITY OF LIBEREC
FACULTY OF TEXTILE ENGINEERING

**WEATHERING OF SIDE EMITTING
POLYMER OPTICAL FIBRES**

Funda Büyük Mazari

Supervisor: doc. Dr. Ing. Dana Křemenáková

Statement

I have been informed that on my thesis is fully applicable the Act No. 121/2000 Coll. about copyright, especially §60 - school work.

I acknowledge that Technical University of Liberec (TUL) does not breach my copyright when using my thesis for internal need of TUL.

Shall I use my thesis or shall I award a license for its utilization I acknowledge that I am obliged to inform TUL about this fact, TUL has right to claim expenses incurred for this thesis up to amount of actual full expenses.

I have elaborate the thesis alone utilizing listed and on basis of consultations with Supervisor.

Date:

Signature:.....

Funda Büyük Mazari

Acknowledgements

This work would have not been possible without the input and guidance of many individuals.

My utmost gratitude to my supervisor, doc. Dr. Ing. Dana Křemenáková, for his patience, guidance and encouragement. Thank you to those that gave me this opportunity and those that helped me along this path.

Lastly and most importantly, to my family and friends; for their endless love and support during this time. Without you'll, it would have not been possible.

Abstract

Side emitting plastic optical fibers (POF) with the trade name of GRACE and HYPOFF with different diameter range were used for evaluating the impact of UV-weathering on tensile properties, bending property and the side emission property. ATLAS weathering machine UV-340 is used for the experiment to evaluate the impact before and after weathering on POF's. It was observed that there is a big loss in terms of tensile and bending properties whereas a minor loss in the side emission property of Plastic optical fiber (POF). Whereas the smaller diameter POF's are more impacted by UV-weathering than the thicker POF's.

Keywords: Optical fibers, polymethyl methacrylate, PMMA, side emission, UV-weathering.

1	INTRODUCTION	14
2	REVIEW	15
2.1	Optical fiber.....	15
2.2	Types of Optical Fibers	15
2.3	Optical Fiber Construction	16
2.4	Total Internal Reflection[7]	17
2.4.1	Reflection of light from optical surfaces.....	17
2.4.2	The law of reflection on plane surfaces:.....	18
2.4.3	Refraction of light from optical interfaces.....	19
2.4.4	Critical angle and total internal reflection	22
2.4.5	Reflection from a curved surface:.....	23
2.5	Chemical composition of optical fibers	24
2.5.1	Polymethyl methacrylate.....	24
2.6	Light intensity Side emission of fibers [18]	26
2.6.1	Principle	26
2.6.2	Description of instrument.....	26
2.7	Weathering.....	28
2.7.1	Factors effecting weathering	28
2.8	Solar Radiation[13].....	29
2.9	Irradiance	29
2.10	SUNLIGHT	30
2.11	WAVELENGTH REGIONS OF THE UV	31
2.11.1	UV-A	31
2.11.2	UV-B	31
2.11.3	UV-C	31
2.12	VARIABILITY OF SUNLIGHT	31

2.13	ACCELERATED LIGHT SOURCES COMPARED TO SUNLIGHT	32
2.14	Radiation components	33
2.15	Radiation energy	33
2.16	The Effect of Radiant Energy on Materials	34
2.17	The Effect of UV on Polymers	35
2.17.1	Photolysis	36
2.17.2	Photo-oxidation	37
2.17.3	UV damage to polymers.....	38
2.18	Importance of short wavelength	39
2.18.1	Light stabilizers for plastic materials.....	39
2.18.1.1	UV light absorbers	40
2.18.1.2	Carbon black.....	40
2.19	Types of Weathering	40
2.19.1	Natural weathering	40
2.19.2	Laboratory Weathering.....	41
2.19.3	Artificial weathering chambers	41
2.20	Fluorescent UV Devices	43
2.21	Tensile properties testing	46
2.22	Flex fatigue of fibers	47
3	EXPERIMENTAL PART	50
3.1	Fiber composition	50
4	METHODOLOGY, RESULTS AND DISCUSSION	51
4.1	Light Intensity side emission comparison	51
4.2	Tensile properties.....	58
4.2.1	Initial Modulus	59

4.2.2	Tensile strength	60
4.2.3	Deformation at break	60
4.2.4	Initial Modulus HYPOFF	62
4.2.5	Deformation at Break HYPOFF.....	62
4.2.6	Tensile strength HYPOFF.....	63
4.3	Bending Rigidity.....	63
4.4	Flexibility	68
4.4.1	SEM pictures	69
5	CONCLUSIONS	70
5.1	Future works	70
6	REFERENCES	71

List of Tables

TABLE 1 INDICES OF REFRACTION FOR COMMON MATERIALS AT 589NM[6].....	20
TABLE 2: MMA CHARACTERISTICS	24
TABLE 3: CHARACTERISTICS OF PMMA	25
TABLE 4 AVERAGE SOLAR RADIATION PER COUNTRY	34
TABLE 5 POF CHARACTERISTICS	50
TABLE 6 WEIBULL PARAMETERS	66

List of Equations

EQUATION 1 INDEX OF REFRACTION.....	16
EQUATION 2 INDEX OF REFRACTION FOR TRANSPARENT MEDIUM.....	19
EQUATION 3 SNELL'S LAW	21
EQUATION 4 SNELL'S LAW.....	22
EQUATION 5 CRITICAL ANGLE.....	23
EQUATION 6 CRITICAL ANGLE OF INCIDENCE.....	23
EQUATION 7 SURFACE LIGHT INTENSITY.....	27
EQUATION 8 ATTENUATION COEFFICIENT.....	27

EQUATION 9 RADIATION ENERGY.....	29
EQUATION 10 STRESS.....	46
EQUATION 11 STRAIN.....	46
EQUATION 12 YOUNG MODULUS.....	47
EQUATION 13 FLEXIBILITY.....	47
EQUATION 14 BENDING CYCLES.....	49
EQUATION 15 BENDING CYCLES TO BREAK.....	49
EQUATION 16 WEIBULL PARAMETER C.....	49
EQUATION 17 WEIBULL PARAMETER A.....	49
EQUATION 18 WEIBULL PARAMETER B.....	49
EQUATION 19 WEIBULL SAMPLE MOMENT.....	49
EQUATION 20 LINEAR FITTING LINE EQUATION.....	56
EQUATION 21 PARAMETERS P0.....	56
EQUATION 22 ATTENUATION COEFFICIENT.....	57

List of Figures

FIGURE 1 STRUCTURE OF A POF [6]	17
FIGURE 2: SPECULAR AND DIFFUSE REFLECTION[7]	18
FIGURE 3 REFLECTION ON A PLANE SURFACE[7]	18
FIGURE 4 REFLECTION AND REFRACTION AT AN INTERFACE[7]	19
FIGURE 5 REFRACTION AT AN INTERFACE BETWEEN MEDIA OF REFRACTIVE INDEXES N1 AND N2[7]	21
FIGURE 6: SNELL'S LAW[6]	21
FIGURE 7: TOTAL INTERNAL REFLECTION	22
FIGURE 8: REFLECTION AT A CURVED SURFACE: ANGLE B EQUALS ANGLE A[6]	24
FIGURE 9: RADICAL FORMATION OF ALKENE ADDITION	25
FIGURE 10: FORMATION OF POLY(METHYL METHACRYLATE).....	25
FIGURE 11: SCHEMATIC DIAGRAM OF PROTOTYPE 1, FOR MEASUREMENT OF SIDE EMISSION.....	26
FIGURE 12 ANGLE OF EXPOSURE TO LIGHT	29
FIGURE 13 THE SUNLIGHT SPECTRUM	30
FIGURE 14 SEASONAL VARIATION OF SUNLIGHT UV	31
FIGURE 15 SOLAR SPECTRUM	32
FIGURE 16 SOLAR SPECTRUM COMPOSITION	33
FIGURE 17 NORRISH I (TOP) AND NORRISH II (BOTTOM)	36

FIGURE 18THE PHOTO-FRIES REARRANGEMENT OF A PHENYL ESTER.....	37
FIGURE 19 PHOTO OXIDATION OF POLYMER[33].....	37
FIGURE 20 NATURAL WEATHERING SOLAR EXPOSURE	41
FIGURE 21 ATLAS UV 2000	44
FIGURE 22 ATLAS UV WORKING	45
FIGURE 23 STRESS,STRAIN CURVE	47
FIGURE 25THE PROTOTYPE BENDING MACHINE	48
FIGURE 24PROTOTYPE INSTRUMENT	48
FIGURE 26COMPARISON OF LIGHT EMISSION AFTER WEATHERING FOR HYPOFF 0.3	51
FIGURE 27COMPARISON OF LIGHT EMISSION AFTER WEATHERING FOR HYPOFF 1	52
FIGURE 28COMPARISON OF LIGHT EMISSION AFTER WEATHERING FOR HYPOFF 1.2	52
FIGURE 29COMPARISON OF LIGHT EMISSION AFTER WEATHERING FOR HYPOFF 1.5	53
FIGURE 30COMPARISON OF SURFACE ILLUMINATION INTENSITY P(Z) HYPOFF.....	53
FIGURE 31COMPARISON OF LIGHT EMISSION AFTER WEATHERING FOR GRACE 0.25.....	54
FIGURE 32COMPARISON OF LIGHT EMISSION AFTER WEATHERING FOR GRACE 0.4.....	54
FIGURE 33COMPARISON OF LIGHT EMISSION AFTER WEATHERING FOR GRACE 0.5.....	55
FIGURE 34COMPARISON OF LIGHT EMISSION AFTER WEATHERING FOR GRACE 0.75.....	55
FIGURE 35COMPARISON OF SURFACE ILLUMINATION INTENSITY P(Z) GRACE.....	56
FIGURE 36LIGHT ATTENUATION COMPARISON FOR GRACE	57
FIGURE 37LIGHT ATTENUATION COMPARISON,HYPOFF	57
FIGURE 38PARAMETER P(0) COMPARISON FOR GRACE.....	57
FIGURE 39 PARAMETER P(0) COMPARISON FOR HYPOFF	57
FIGURE 40STRESS-STRAIN MEAN CURVE (GRACE 0.25).....	58
FIGURE 41STRESS-STRAIN MEAN CURVE (GRACE 0.5).....	58
FIGURE 42STRESS-STRAIN MEAN CURVE (GRACE 1).....	59
FIGURE 43MEAN INITIAL MODULUS COMPARISON (GRACE)	59
FIGURE 44MEAN TENSILE STRENGTH COMPARISON (GRACE)	60
FIGURE 45MEAN DEFORMATION AT BREAK COMPARISON (GRACE).....	60
FIGURE 46STRESS-STRAIN MEAN CURVE (HYPOFF 1.2).....	61
FIGURE 47STRESS-STRAIN MEAN CURVE (HYPOFF 1.5).....	61
FIGURE 48MEAN INITIAL MODULUS COMPARISON (HYPOFF)	62
FIGURE 49 MEAN DEFORMATION AT BREAK (HYPOFF).....	62

FIGURE 50MEAN TENSILE STRENGTH COMPARISON (HYPOFF).....	63
FIGURE 51BENDING CYCLES TO BREAK GRACE.....	63
FIGURE 52WEIBULL PROBABILITY PLOT (GRACE0.25)	64
FIGURE 53WEIBULL PROBABILITY PLOT (GRACE 0.25AFTER WEATHERING)	64
FIGURE 54BENDING CYCLES TO BREAK(HYPOFF).....	65
FIGURE 55WEIBULL PROBABILITY PLOT (GRACE 0.3)	65
FIGURE 56WEIBULL PROBABILITY PLOT (GRACE 0.3 AFTER WEATHERING)	66
FIGURE 57WEIBULL PARAMETER A,GRACE.....	67
FIGURE 58WEIBULL PARAMETER A,HYPOFF.....	67
FIGURE 59FLEXIBILITY COMPARISON GRACE.....	68
FIGURE 60FLEXIBILITY COMPARISON HYPOFF	68
FIGURE 61 0.25 GRACE BEFORE WEATHERING.....	69
FIGURE 62 0.25 GRACE AFTER WEATHERING	69
FIGURE 63HYPOFF 1.2 AFTER WEATHERING	69
FIGURE 64HYPOFF 1.2 BEFORE WEATHERING	69
FIGURE 65HYPOFF 1.5 AFTER WEATHERING	69
FIGURE 66HYPOFF 1.5 BEFORE WEATHERING	69

LIST OF SYMBOLS

A [cycles]	lowest number of repeating bending cycles to break
B [cycles]	scale parameter
C [-]	shape parameter
c [m/s]	speed of light in a vacuum
d [mm]	diameter of the circle
D _B [%]	deformation at break
E [Pa]	youngs modulus
F [N]	force
F _e [N ⁻¹ mm ⁻²]	flexibility

FC_M [cycle]	the mean value of repeating bending cycles to break
h [$m^2 \text{ kg/s}$]	Plank's constant
L [m]	length of the material
l [$^\circ$]	angle of incidence
n [-]	index of refraction of the medium
n_i [-]	index in the incident medium
n_r [-]	index in the refracting medium
i_c [$^\circ$]	critical angle of incidence
r [$^\circ$]	angle of refraction
ΔL [-]	change in the length of the material
σ [Pa]	stress
UV [nm]	ultraviolet rays
RH [%]	relative humidity
v [m/s]	speed of the light in the medium
λ [nm]	wave length
ε [-]	strain
α	attenuation coefficient of optical fiber
SPD	spectral power distribution
PMMA	Polymethyl methacrylate
POF	Plastical optical fiber
$P(z)$ [W/m^2]	light illumination intensity
z [m]	distance from light source

1 Introduction

Plastic optical fiber (POF) has received a lot of interests, which is expected to be a communication medium of next generation. The recent large demand for the construction of huge optical telecommunication networks has been a stimulating intense development in the field of communication medium [1]. But POF has also another great use as side emitting optical fibers where it can be used in textile stuff and can be part of the weave or can be bonded at required places for illumination at specific places, The uses of side emitting fibers in textile would prove to be beneficial in several ways, few of them being the flexibility of the fiber for integration into fabrics. Uses of side emitting optical fibers could be for

- Night jackets for emergency personal (police, fireman, paramedics)
- Integration into clothing of cyclists and runners for night use
- Emergency illumination of stairways and emergency exits in buildings
- Illumination strip on car doors if they are open
- Fashion

To clearly know the future of optical fibers we must know how long and well it will behave under different conditions. Sunlight is an important cause of damage to plastics, textiles, paints, and other organic materials. Short wavelength ultraviolet light has long been recognized as being responsible for most of this damage [2,3]. So major properties like mechanical properties, light emission ability and bending property have to be tested under accelerated weathering to determine all these properties after weathering and how long optical fibers can perform under normal environment condition. so in this research impact of UV-weathering will be tested for different properties of POF's

2 Review

2.1 Optical fiber

Optical fibers have a very broad spectrum of use, ranging from transporting light from a source to some device, transmitting optically encoded data or even functioning as a sensor for temperature or strain [3].

Most fibers are used to guide light, and since optical fibers have the ability to keep the light inside the fiber, this is advantageous. The fiber does this by internally reflecting the light in the core of the fiber, along the fiber axis. These principles will be discussed in the subsequent sub-chapters.

2.2 Types of Optical Fibers

Principally there are three types of optical fibers used in telecommunications; the type off course is dependent on its use and the final application. The three types can be further split into two categories, namely single and multi-mode fibers [4].

- Step-index multi-mode fiber
- Graded-index multi-mode fiber
- Single-mode fiber

Single-mode, or also known as mono-mode fiber is approximately 8-10 μ m in diameter [5] and has only one mode of transmission, i.e. the signal or light wave will travel in only one direction, which is linear. Having a smaller diameter, the fiber requires a light source with a narrow spectral width. This fiber is used when the signal required has to transmit at a higher rate, and for longer distances. The reason for the ability to transmit over longer distances is because of the single light wave and the small core, which eliminates most distortion in the signal. The typical wavelengths transmitted using single-mode fibers are between 1310-1550nm.

In comparison to single-mode fibers, multi-mode fibers have a typical diameter range of 50-100 μ m. The functions are principally the same, for primarily for light transmission

which is converted into a signal, but the multi-mode fibers are able to process more light, at high speeds. The light waves are dispersed into a number of paths, and due to this, long lengths of multi-mode fibers are not possible due to interference within the line. The other major factor is that multi-mode fibers do not require a light source of narrow spectral width and thus are able to transmit light of lower wavelengths (850nm) in comparison to the single-mode fibers.

2.3 Optical Fiber Construction

A single optical fiber is made up of several components and these include the

- Core
- Cladding
- Coating buffer
- Strength member
- Outer jacket

The core is the light carrying element, whereas the cladding assists in total internal reflection. This is achieved by using a cladding which has a lower refractive index as compared to the core, causing the light transmitted in the core to reflect off the cladding and remain within the core. The refractive index can be described as the ratio between the velocity of light in vacuum and the velocity of light in the material. Thus the higher the refractive index, the slower the speed of light through the material.

$$\text{Index of Refraction} = \frac{\text{Light velocity}_{\text{vacuum}}}{\text{Light velocity}_{\text{material}}} \quad (1)$$

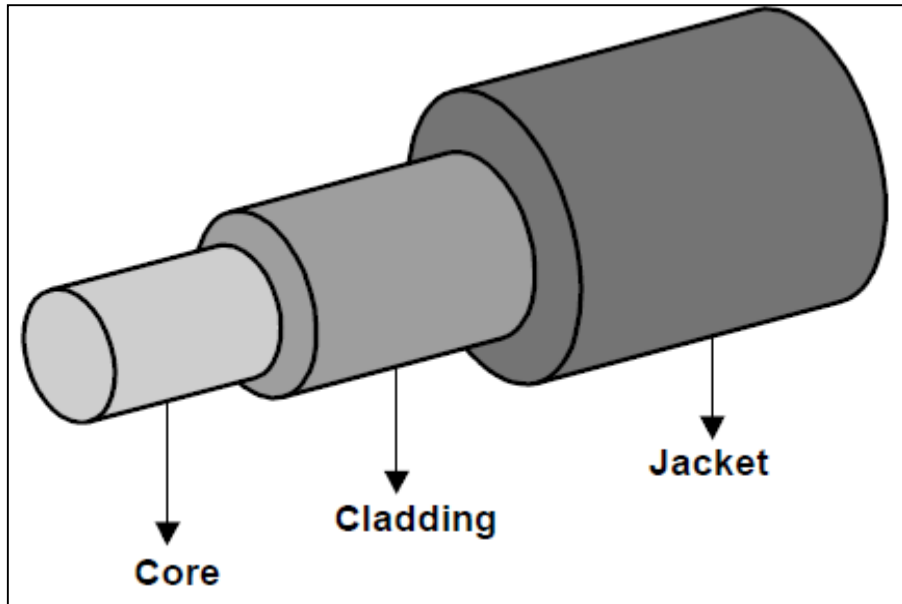


Figure 1 Structure of a POF [6]

2.4 Total Internal Reflection[7]

Optical fibers function well because of its ability to keep the light within the fiber core. When light travels from one material to another of different density[8], the light's path will bend. At a particular point, or rather angle the light will not pass through the surface, but instead bounce off the surface. Optical fibers make use of this phenomenon to bend light at its boundary, which is the cladding, and trap the light within the core. Thus by selecting material differences i.e. different refractive indices between the core and cladding, it is possible to select the angle at which total internal reflection occurs.

2.4.1 Reflection of light from optical surfaces

When light is incident on an interface between two transparent optical media, such as between air and glass or between water and glass, four things can happen to the incident light.

- It can be partly or totally reflected at the interface.
- It can be scattered in random directions at the interface.
- It can be partly transmitted via refraction at the interface and enter the second medium.

- It can be partly absorbed in either medium.

In the case of Optical Fibers, the surfaces are smooth, and thus the rough surfaces can be ignored[6].

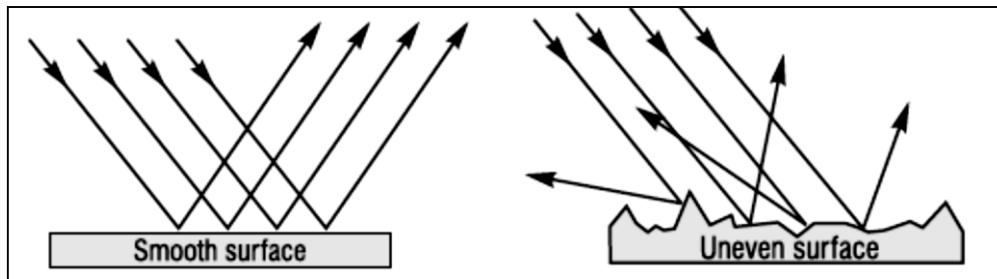


Figure 2: Specular and diffuse reflection[7]

2.4.2 The law of reflection on plane surfaces:

When light reflects from a plane surface (*Figure 3*), the angle that the reflected ray makes with the normal (line perpendicular to the surface) at the point of incidence is always equal to the angle the incident ray makes with the same normal. Important to note is that the incident ray, reflected ray, and normal lie in the same plane.

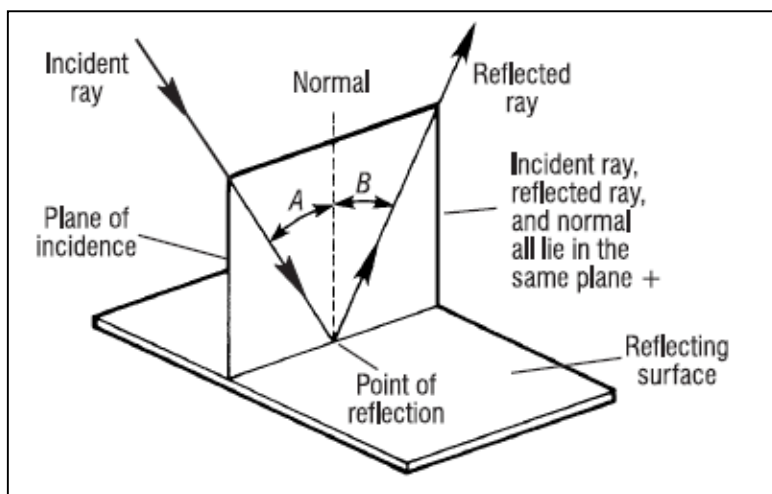


Figure 3 Reflection on a plane surface[7]

2.4.3 Refraction of light from optical interfaces

When light is incident at an interface, the geometrical plane that separates one optical medium from another, it will be partly reflected and partly transmitted. *Figure 4* shows a three-dimensional view of light incident on a partially reflecting surface (interface), being reflected there (according to the *law of reflection*) and refracted into the second medium. The bending of light rays at an interface between two optical media is called *refraction*.

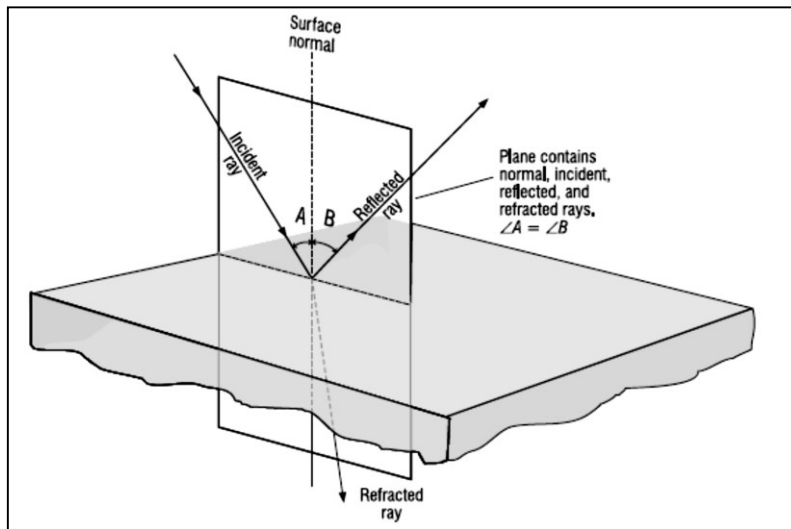


Figure 4 Reflection and refraction at an interface[7]

Index of refraction: The two transparent optical media that form an interface are distinguished from one another by a constant called the *index of refraction*, generally labelled with the symbol n . The index of refraction for any transparent optical medium is defined as the ratio of the speed of light in a vacuum to the speed of light in the medium, as given in

$$n = \frac{c}{v} \quad (2)$$

where

c = speed of light in free space (vacuum)

v = speed of light in the medium

n = index of refraction of the medium

The index of refraction for free space is exactly *one*. For air and most gases it is very nearly one, hence in most calculations it is taken to be 1.0. For other materials it has values greater than one.

Table 1 Indices of refraction for common materials at 589nm[6]

Substance	<i>n</i>	Substance	<i>n</i>
Air	1.0003	Quartz (fused)	1.46
Glass (flint)	1.66	Diamond	2.42
Benzene	1.50	Sodium Chloride	1.54
Glycerin	1.47	Ethyl Alcohol	1.36
Carbon Disulfide	1.63	Water	1.33
Polystyrene	1.49	Gallium Arsenide	3.40
Corn Syrup	2.21	Ice	1.31

The greater the index of refraction of a medium, the lower the speed of light in that medium and the more light is bent in going from air into the medium. *Figure 5* shows two general cases, one for light passing from a medium of lower index to higher index, the other from higher index to lower index. Note that in the first case (lower-to-higher) the light ray is bent toward the normal. In the second case (higher-to-lower) the light ray is bent away from the normal.

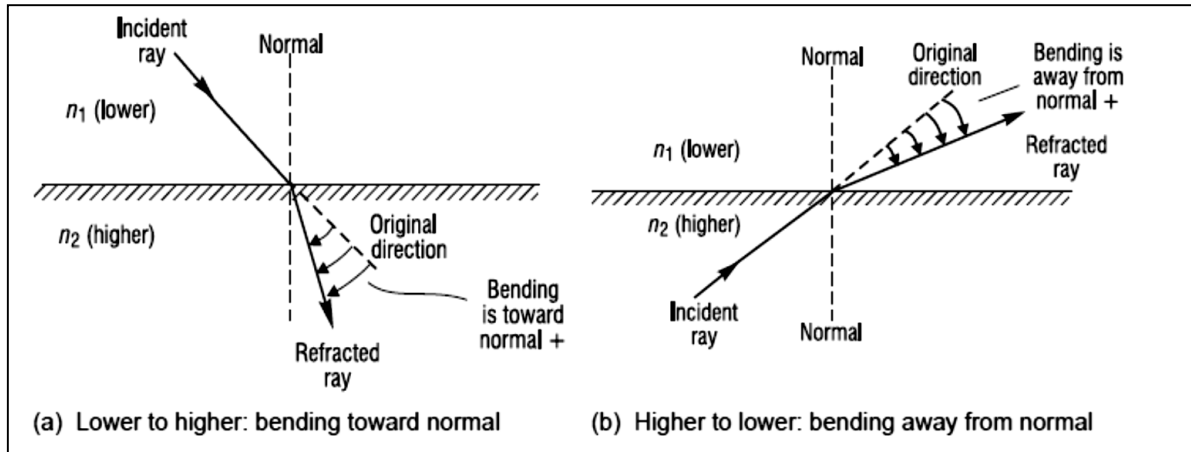


Figure 5 Refraction at an interface between media of refractive indexes n_1 and n_2 [7]

Snell's law

Snell's law of refraction relates the sines of the angles of incidence and refraction at an interface between two optical media to the indexes of refraction of the two media. The law is named after a Dutch astronomer, Willebrord Snell[9], who formulated the law in the 17th century. Snell's law enables us to calculate the direction of the refracted ray if we know the refractive indexes of the two media and the direction of the incident ray.

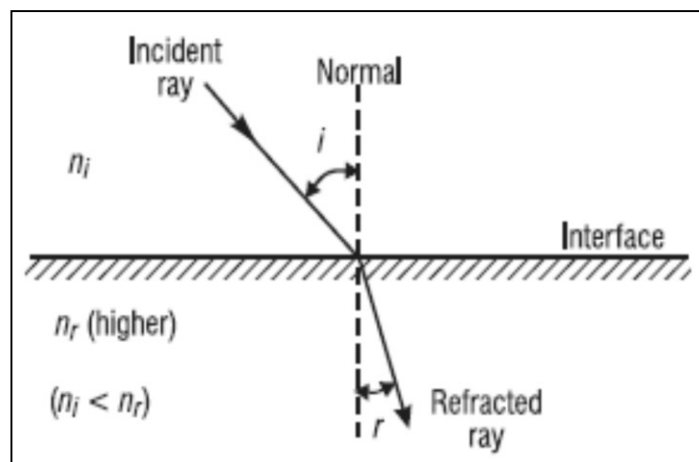


Figure 6: Snell's Law[6]

$$\frac{\sin i}{\sin r} = \frac{n_r}{n_i} \quad (3)$$

Where,

i is the angle of incidence

r is the angle of refraction

n_i is the index in the incident medium

n_r is the index in the refracting medium

Snell's law is often written simply as

$$n_i \sin i = n_r \sin r \quad (4)$$

2.4.4 Critical angle and total internal reflection

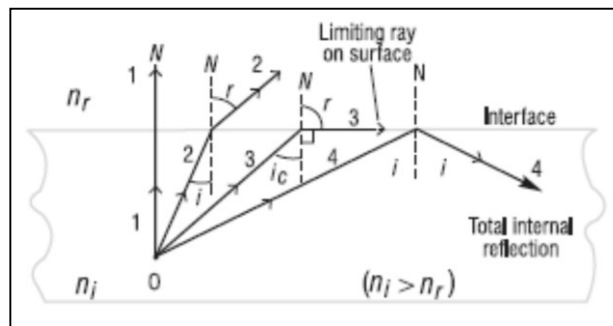


Figure 7: Total internal reflection

Figure 7, Shows four rays of light originating from point O in the higher-index medium, each incident on the interface at a different angle of incidence. Ray 1 is incident on the interface at 90° (normal incidence) so there is no bending. The light in this direction speeds up in the second medium but continues along the same direction. Ray 2 is incident at angle i and refracts (bends away from the normal) at angle r . Ray 3 is incident at the *critical angle* i_c , large enough to cause the refracted ray bending away from the normal (N) to bend by 90° , thereby traveling along the interface between the two media. (This ray is trapped in the interface.) Ray 4 is incident on the interface at an angle *greater than* the critical angle, and is *totally reflected* into the same medium from which it came. Ray 4 obeys the *law of reflection* so that its angle of reflection is exactly equal to its angle of incidence. The phenomenon of total internal reflection is exploited when designing light propagation in fibers[6] by trapping the light in the fibre through successive internal reflections along the

fiber. In comparison to ordinary reflection from mirrors, the sharpness and brightness of totally internally reflected light beams is enhanced.

The calculation of the critical angle of incidence for any two optical media whenever light is incident from the medium of higher index is accomplished with *Snell's law*. Referring to Ray 3 in *Figure 7* and using Snell's law appropriately, we have

$$n_i \sin i_c = n_r \sin 90^\circ \quad (5)$$

where n_i is the index for the incident medium, i_c is the critical angle of incidence, n_r is the index for the medium of lower index, and $r = 90^\circ$ is the angle of refraction at the critical angle. Then, since $\sin 90^\circ = 1$, we obtain for the critical angle,

$$i_c = \sin^{-1} \left(\frac{n_r}{n_i} \right) \quad (6)$$

This phenomenon explains the principles of the functioning of optical fibres.

2.4.5 Reflection from a curved surface:

With spherical mirrors, reflection of light occurs at a curved surface, and this principle is similar to that in optical fibres. The Law of reflection holds, since at each point on the curved surface one can draw a tangent and erect a normal to a point P on the surface where the light is incident, as shown in *Figure 8*. One then applies the *law of reflection* at point P just as was illustrated in *Figure 4*, with the incident and reflected rays making the same angles (A and B) with the normal to the surface at P . Note that successive surface tangents along the curved surface in *Figure 8* are ordered (not random) sections of “plane mirrors” and serve, when smoothly connected, as a spherical surface mirror, capable of forming distinct images.

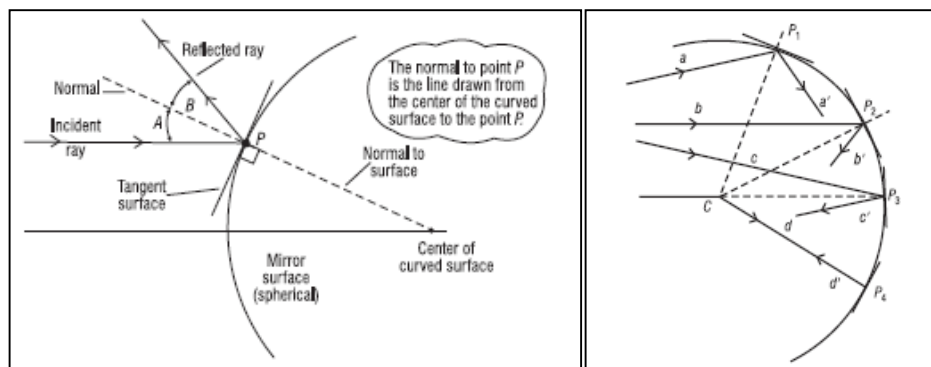


Figure 8: Reflection at a curved surface: Angle B equals angle A[6]

Since point P can be moved anywhere along the curved surface and a normal drawn there, we can always find the direction of the reflected ray by applying the *Law of reflection*.

2.5 Chemical composition of optical fibers

Plastic optical fibers have been manufactured from a number of transparent polymers such as Polymethyl methacrylate(PMMA), polystyrene(PS), polycarbonate(PC), CYTOP (amorphous fluorinated polymer), hard core silica(HCS), and plastic clad silica(PCVS)[9]

2.5.1 Polymethyl methacrylate

Table 2: MMA characteristics

	Methyl methacrylate[14]	
	Chemical Formula	$C_5H_8O_2$
	Molar mass	$100.12 \text{ g} \cdot \text{mol}^{-1}$
	Density	$0.94 \text{ g} \cdot \text{cm}^3$
	Melting point	-48°C , 225K
	Boiling point	101°C , 374K

Methyl acrylate is the monomer of Poly(methyl methacrylate), and the polymer is formed by the simple addition of alkenes, the reaction was adapted from Clayden, Organic chemistry[10]

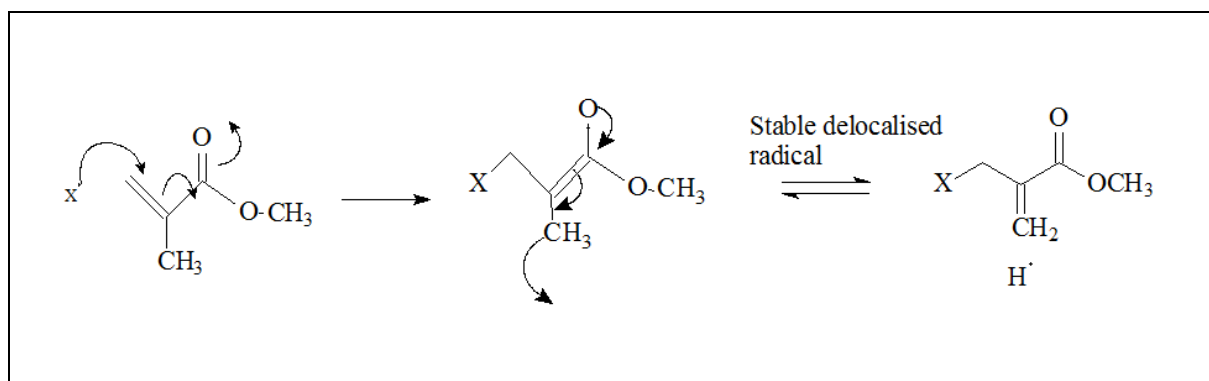


Figure 9: Radical formation of alkene addition

After the radical formation, the polymer can be easily formed by the following

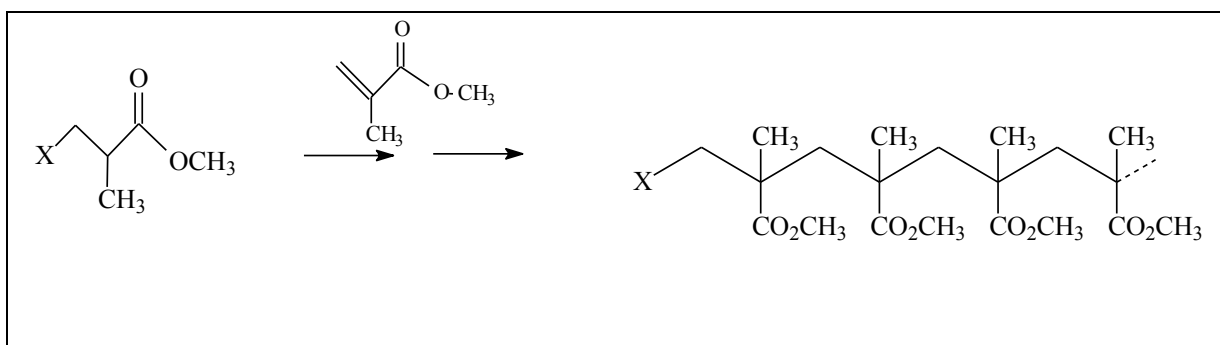


Figure 10: Formation of Poly(methyl methacrylate)

Table 3: Characteristics of PMMA

	Poly(methyl methacrylate)[10]	
	Molecular Formula	(C ₅ H ₈ O ₂) _n
	Density	1.18 g/cm ³
	Melting point	160°C, 433K
	Boiling point	200°C, 473K
	Refractive index	1.4914 at 587.6nm

Poly(methyl methacrylate) is known as PMMA. It is a strong and light weight material, with a density half of that of glass (density of glass is between 2.4 -2.8 g/cm³)[11]. It also has good impact strength when compared to glass and polystyrene.

PMMA transmits up to 92% of visible light, and gives a reflection of about 4% due to its refractive index. The maximum water absorption ratio is 0.3 to 0.4% by weight, thus the polymer is highly hydrophobic.

2.6 Light intensity Side emission of fibers [18]

2.6.1 Principle

The device is intended for guiding laterally emitting optical fiber or a textile structure which contains optical fibers and to measure the light output that these structures emit. The optical fiber or textile structure is located between the feed rollers, which guide them to the measuring tunnel, where there is a single measurement of light output. The tow rollers are driven by step motor. After guiding the thread through the device, the thread is illuminated. The actual measurement is performed with the use of a light sensor, which reads the light output in pre-defined step lengths. Step lengths are processed by a step motor that drives the tow rollers. The actual device is controlled by a computer program created in MATLAB.

2.6.2 Description of instrument

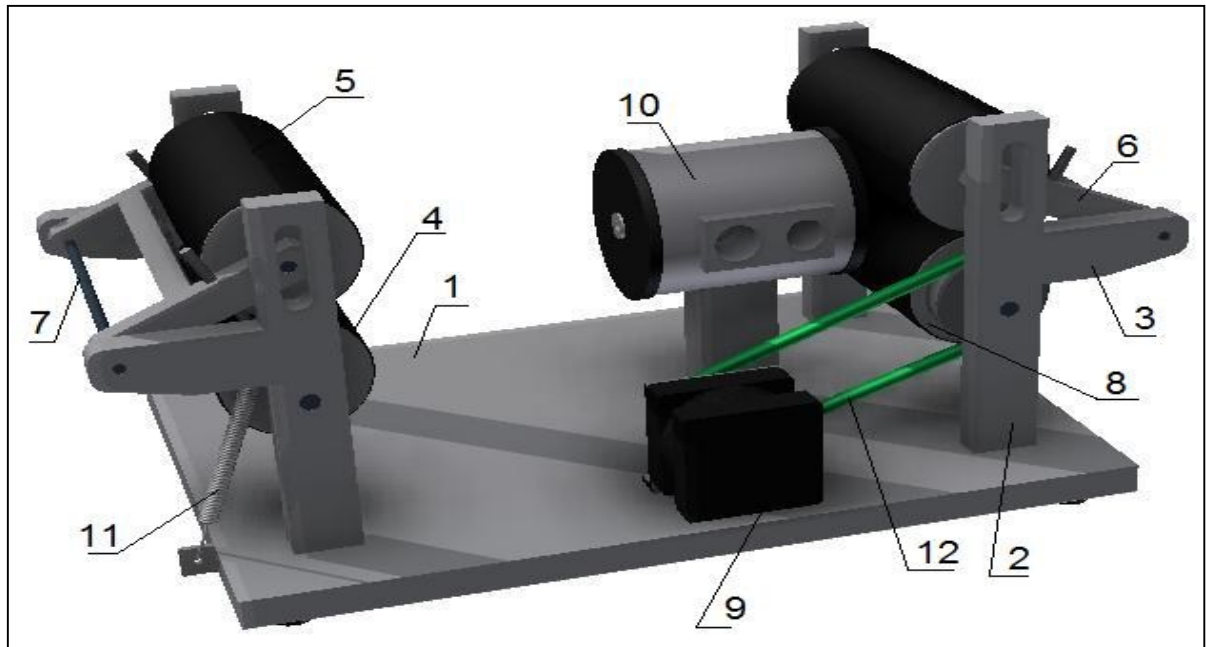


Figure 11: Schematic diagram of Prototype 1, for measurement of side emission

Referring to the above diagram, the device consists of a base plate (1). This plate is fastened on the edges of four columns (2), among which are fixed free (4) and pressure (5) rollers for feeding and extraction of fibers. The poles are brackets (3), which are mounted with the pressure roller which works as a shaft lever (7). It allows manipulation of the rollers. The actual pressure roller is placed on the push lever (6), the intensity of pressure that develops through two tension springs (11). Alongside the bottom roller (driving roller) (8) is a fixed drive belt (12) which is powered by a step motor (9). The middle measuring tunnel is mounted onto the base plate (10). It is equipped with two lids in order to avoid measurement bias. In addition, the measurement tunnel contains two holes to fix a spectrometer and a light sensor.[42]

Due to the transmission loss, the power of radiation emitted in any direction decays exponentially along the fiber axis with increasing distance from the light source of the fiber as observed by Zajkowski [27], while the percentage of light emitted per unit length is uniform over the entire fiber length. The simple model for prediction of this attenuation is proposed. Illumination power $P(z)$ [W/m²] is decreasing for straight optical fiber with increasing distance from source z according to relation [28].

$$P(z) = P(0) \cdot 10^{-\alpha z/10} \quad (7)$$

where $P(0)$ is illumination intensity of source that quality of illumination system and α is attenuation coefficient of optical fiber which is fiber quality characteristic

Coefficient α describes attenuation value at dependence of fiber length.

$$\alpha = \frac{-10}{z} \log \left(\frac{P(z)}{P(0)} \right) \quad (8)$$

2.7 Weathering

Weathering is the adverse response of a material or product to climate, often causing unwanted and premature product failures. Consumers spend billions of dollars per year to maintain products that inevitably degrade and to replace products that fail. Materials that fail as a result of exposure to outdoor environments account for a significant portion of this total cost.

Most materials are subject to weathering. The earth's crust is degraded by chemical and physical processes as a result of exposure to the elements. The rate of deterioration depends on the nature of the material; for the hardest rock the time scale stretches to millions of years whereas for some organic polymers major changes can be induced by exposures of few days

Synthetic polymers offer an impressive range of attractive properties and in many of their applications they are exposed to the outdoor environment. For example; polymers and composites are widely used externally as well as internally in aircraft, in boat construction and in the building industry plastics, composites and synthetic fibers are displacing more conventional materials

Whatever the application; there is often a natural concern regarding the durability of polymeric materials partly because of their relative newness but also because of the useful lifetime of these material can be predicted their maintenance and replacement can be planned [29]

2.7.1 Factors effecting weathering

The three main factors of weathering are solar radiation (light energy), temperature, and water (moisture). But it is not just “how much” of each of these factors ultimately causes degradation to materials, because different types of solar radiation, different phases of moisture, and temperature cycling have a significant effect on materials on exposure. These factors, in conjunction with secondary effects such as airborne pollutants, biological phenomena, and acid rain, act together to cause “weathering.”

- Water
- Pollution
- Temperature
- Sunlight

- Physical interaction
- Impurities in air

2.8 Solar Radiation[13]

Radiant energy that comes from the sun is made up of photons that travel through space as waves. Their energy (E) is proportional to their frequency (v) according to the following equation, where (h) is Planck's constant, (c) is the velocity of light in a vacuum, and (λ) is wavelength.

$$E = hc/\lambda \quad (9)$$

- Ultraviolet (UV)- 295 – 400 nm, 6.8% of Total Solar
- Visible (VIS)- 400 – 800 nm-55.4% of Total Solar
- Infrared (IR) 800 – 2450 nm-37.8% of Total Solar

2.9 Irradiance

Irradiance can be defined as the radiant flux incident on a surface per unit area, commonly expressed in W/m². For this parameter, it is necessary to indicate the spectral range in which the measurements were taken or for which the values were calculated, such as 295-3000 nm (total solar) or 295-400 nm (total UV). If we turn our attention to narrow wavelength intervals, we obtain the spectral irradiance, measured in W/m²/nm. For weathering tests, the concept of radiant exposure, which is the time integral of (spectral) irradiance, may be more important, stated in J/m². Most radiant exposures are measured in either kJ/m² or MJ/m² to convert this energy into numbers to which we can more easily relate.

The percentage of direct, diffuse, and reflected radiation striking a material is determined by the angle of exposure, as well as the atmospheric conditions.

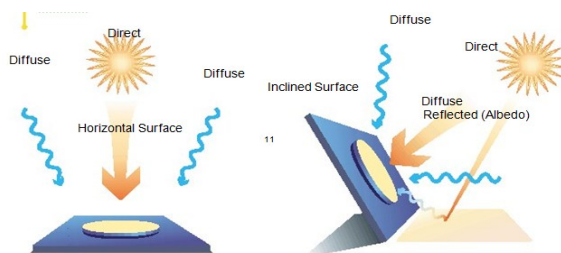


Figure 12 Angle of Exposure to light

The solar radiation that reaches the earth's surface consists of wavelengths between 295 and 3000 nanometers. A nanometer is one billionth (1×10^{-9}) of a meter. This terrestrial sunlight is commonly separated into three main wavelength ranges: ultraviolet (UV), visible (VIS), and infrared (IR). Wavelengths between 295 and 400 nm are considered the ultraviolet (UV) portion of the solar spectrum, making up between 4–7% of the total radiation. Ozone in the stratosphere absorbs and essentially eliminates all radiant energy below 295 nm. Extremely sensitive instruments may detect radiation below 295 nm, but this amount is considered negligible by most experts.

2.10 SUNLIGHT

The electromagnetic energy from sunlight is normally divided into ultraviolet light, visible light, and infrared energy. Figure(13) below shows the spectral power distribution (SPD) of noon midsummer sunlight, measured in Cleveland Ohio, June, 1986[14,15]. Infrared energy (not shown) consists of wavelengths longer than the visible red wavelengths and starts above about 760 nanometers (nm). Visible light is defined as radiation between 400 and 760 nm. Ultraviolet light consists of radiation below 400 nm. The International Commission on Illumination (CIE) further subdivides the UV portion of the spectrum into UV-A, UV-B and UV-C as shown below

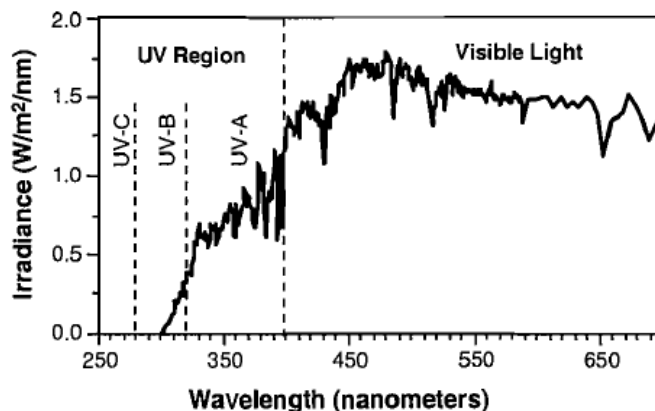


Figure 13 The sunlight spectrum

The effects of the various UV wavelength regions can be summarized as shown in the following

2.11 WAVELENGTH REGIONS OF THE UV

2.11.1 UV-A

400 to 315 nm-Causes polymer damage

2.11.2 UV-B

315 to 280 nm-Includes the shortest wavelengths found at the earth's surface; responsible for severe polymer damage; absorbed by window glass.

2.11.3 UV-C

280 to 100 nm-Found only in outer space; filtered out by earth's atmosphere.

2.12 VARIABILITY OF SUNLIGHT

Because UV is easily filtered by air mass, cloud cover, pollution, etc., the amount and spectrum of natural UV exposure is extremely variable. Figure 14, shows a comparison of the UV regions of sunlight, measured at Cleveland at noon on: The summer solstice (longest day of the year), The winter solstice (shortest day of the year), The spring equinox, These measurements are in essential agreement with data reported by other investigators[16]. Because the sun is lower in the sky during the winter months, it is filtered through a greater air mass. This creates two important differences between summer and winter sunlight: changes in the intensity of the light and in the spectrum. Most important, the shorter, more damaging UV wavelengths are filtered out during winter. For example, the intensity of UV at 320 nm changes about 8 to 1 from summer to winter. This is especially significant for polymeric materials such as PVC. In addition, the short wavelength solar cut-off shifts from about 295 nm in summer to about 310 nm in winter. Consequently, materials sensitive to UV below 310 nm would degrade only slightly, if at all, during the winter months. The sunlight spectrum at the March 21 equinox falls between the June and December curves.

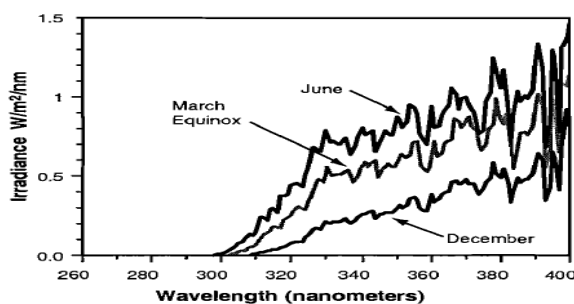


Figure 14 Seasonal Variation of Sunlight UV

2.13 ACCELERATED LIGHT SOURCES COMPARED TO SUNLIGHT

The following discussion of light sources will confine itself to the question of UV spectrum. It will not address problems of light stability, the effects of moisture and humidity, the effects of cycles, or the reproducibility of results. For simulations of direct sunlight, artificial light sources should always be compared to what we will call the Solar Maximum condition: global, noon sunlight, on the summer solstice, at normal incidence. 'The Solar Maximum is the most severe condition met in outdoor service, and as such it controls which materials will fail. It is misleading to compare light sources against so-called "average optimum sunlight", which is simply an average of the much less damaging March 21 and September 21 equinox readings. Graphs labeled "sunlight" in this paper refer to the Solar Maximum - noon, global, midsummer

Ultraviolet light spectrum and solar radiation

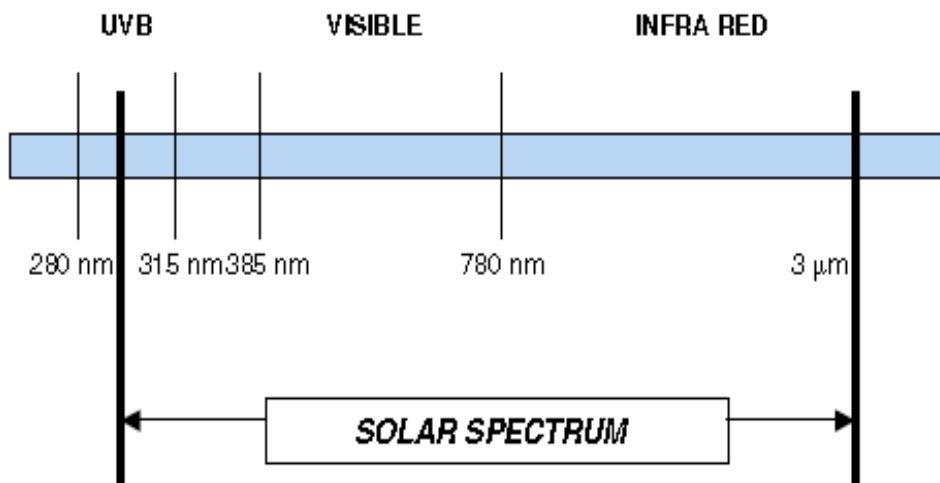


Figure 15 Solar spectrum

2.14 Radiation components

UV radiation represents only 4.6% of the solar spectrum, but causes the most important damage to the polymeric materials. The complete solar UV spectrum ranges between 280 and 400 nanometers, but the most aggressive part is the UVB range with very short wavelengths

between 280 and 315 nanometers.

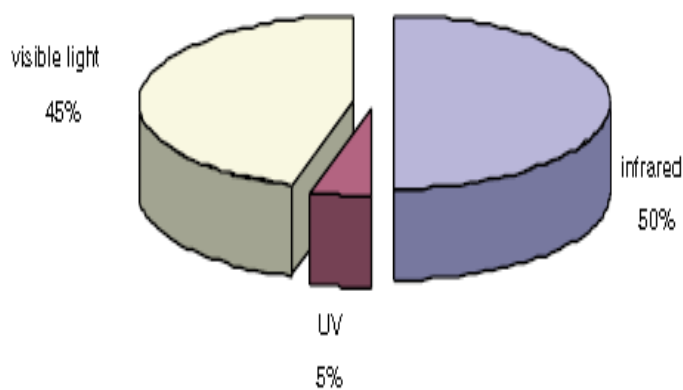


Figure 16 Solar spectrum Composition

2.15 Radiation energy

The **irradiation** is the radiation energy incident over a specific area for a given period of time. It is expressed either in

W*s /m², Joule/m²

or very often in **Langley (Ly)**.

1 Ly = 1 cal/cm² = 4.184 E⁴Joule/m²

➤ annual sunlight radiation in Belgium : 80 kLy (see table below)

➤ total irradiation after 3 years : 80 x 3 = 240 kLy

The global annual sunlight radiation level (kLy/year) for various countries is given in the table below. It corresponds to the radiation energy that can be transmitted to a plastic part in one year of continuous outdoor exposure.

Table 4 Average solar radiation per country

COUNTRY	kLy	COUNTRY	kLy	COUNTRY	kLy	COUNTRY	kLy
Austria	80	Germany	80	Morocco	160	Suriname	120
Afghanistan	180	Great Britain	70	Mauritania	180	Sweden	70
Alaska	70	Greece	120	Mexico	160	Switzerland	80
Algeria	160	Guatemala	140	Mozambique	160		
Angola	120	Guyana	120			Taiwan	140
Argentina	160			Nepal	160	Thailand	140
Australia	180	Haiti	160	Netherlands	80	Tunisia	160
		Hong Kong	140	Nicaragua	140	Turkey	140
Bahamas	140	Honduras	140	Niger	200		
Bahrain	200	Hungary	80	Norway	70	Uruguay	160
Belgium	80			New Zealand	120	USA	
Burma	120	India	180			North	100
Bolivia	140	Indonesia	140	Oman	160	Arizona	180
Brazil	120	Iraq	180			Florida	140
Bulgaria	100	Iran	180	Pakistan	180	Uganda	140
		Israel	180	Panama	40		
Canada	100	Italy	120	Paraguay	160	Vietnam	140
Chad	200	Jamaica	160	Peru	140	Venezuela	160
Chile	140	Japan	100	Philippines	140		
China	140	Jordan	180	Poland	80	Zambia	180
Columbia	100			Portugal	40		
Costa Rica	140	Kenya	140	Rumania	100		
Cuba	140	Kuwait	180	Russia (North)	70		
Cyprus	140	Korea	120	Russia (South)	140		
Denmark	70	Lebanon	180	Sardinia	20		
		Luxembourg	80	Saudi Arabia	200		
Egypt	200	Libya	180	Senegal	180		
Ecuador	120			Sicily	140		
El Salvador	140	Madagascar	140	Singapore	140		
Ethiopia	140	Mali	200	South Africa	160		
		Malta	160	Spain	140		
Finland	70	Malaysia	140	Sudan	220		
France	120						

2.16 The Effect of Radiant Energy on Materials

While radiant exposure is an important factor in understanding the degradation of materials or determining the length of a weathering test, it really tells us only half the story. Radiant exposure tells only how much radiation has been deposited onto the surface of a material. It says nothing about how much of that radiation has been absorbed by the material.

According to the Grotthus-Draper principle,

Absorption of radiation by any component of the system is the first necessary event for photochemical reaction.

To put this in layman's terms, "If radiation can get into a material, it potentially can cause it to change." But does this mean that a black paint will degrade in the sun because it is absorbing nearly all wavelengths of visible light? The answer to that question lies in

understanding the chemical nature of the paint and which wavelengths of radiation will cause this paint to degrade.

The molecular structures that constitute different polymers are susceptible to radiation they might absorb. Following another basic principle of degradation, The amount of energy absorbed by a molecule must exceed the bond energy to cause degradation. Simply put, if the absorbed radiation has more energy than the energy holding the molecular structure together, polymeric bonds will be altered and degradation will begin. As previously discussed, we know that shorter wavelengths contain higher amounts of energy. Therefore, it is now easy to understand, when we are discussing the durability of a material, why UV, as the shortest wavelength region of radiation to reach the earth's surface, is the most important part of sunlight. It has been found through experimentation that a certain plastic absorbs radiant energy and degrades when irradiated below 310 nm.

2.17 The Effect of UV on Polymers

It has been stated that, the UV radiation is one of the most important factors determining the polymers lifetime.[29,30] Degradation due to UV radiation is called photodegradation. Chemical reactions (e.g. chain scissions, cross linking, and oxidation) influence the physical properties and thus the material's lifetime.[31]

When light is absorbed by a polymer, photochemical reactions can occur as a result of activation of a polymer macromolecule to its excited singlet or triplet states. If the energy of the absorbed UV light is higher than the bond energy, the chemical bond may break.

The most important mechanisms causing weathering of polymers are photolysis and photo oxidation.[32] If the absorption of light leads directly to chemical reactions causing degradation, this is called photolysis. Photo-oxidation is a result of the absorption of light that leads to the formation of radicals that induces oxidation of the material.

For these polymers in principle there are three mechanisms that can describe their light-induced degradation:

- Photolysis; absorption as a result of the inherent polymeric structure results in chemistry causing changes in the molecular structure;
- Photo-oxidation initiated by photolysis reactions of the polymer itself as mentioned above;

- Photo-oxidation initiated by impurities not part of the inherent polymer structure.[30]

2.17.1 Photolysis

Photolytic reactions occur when light is absorbed by the polymer and leads to changes in structure. Important photolytic reactions for degradation are the Norrish I and Norrish II reactions and the photo-Fries rearrangement.

When light is absorbed by the polymer, Norrish reactions can occur, which lead to changes in molecular structure resulting in degradation.[32] The Norrish I reaction leads to chain cleavage and radicals that might initiate the photo-oxidation. The Norrish II reaction is a non-radical intermolecular process, in which hydrogen is transferred, leading to chain cleavage. For polyamides and polyesters the most important photolytic reactions are the Norrish I and II reactions. In Figure 17 both reactions are shown.

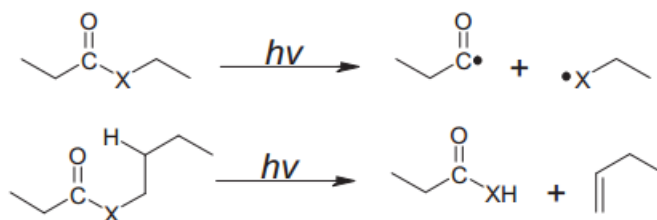


Figure 17 Norrish I (top) and Norrish II (bottom)

Norrish I (top) and Norrish II (bottom) reactions for polyamides (X=NH) and polyesters (X=O).

Engineering plastics containing phenyl ester groups, like polycarbonates, can undergo Fries rearrangements. When a phenyl ester rearranges, as a result of the absorption of UV radiation, it is called the photo-Fries rearrangement. In Figure 18 the photo-Fries rearrangement of a phenyl ester is shown. The reaction involves three basic steps; 1) the formation of two radicals, 2) recombination, and 3) hydrogen abstraction.

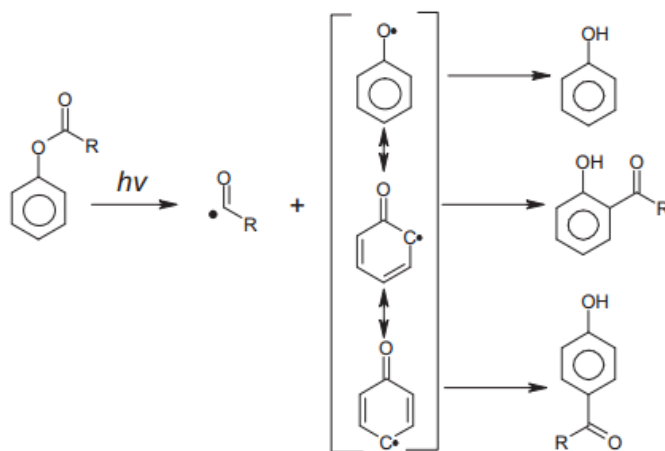
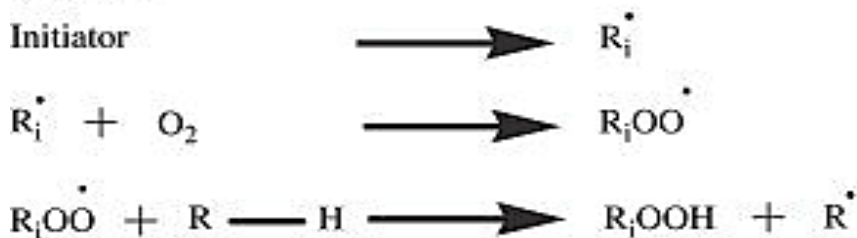


Figure 18 The photo-Fries rearrangement of a phenyl ester

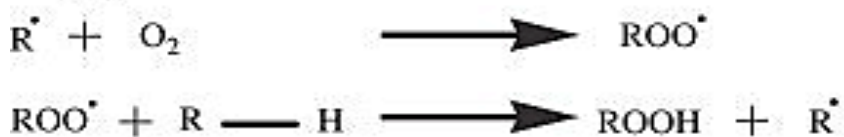
2.17.2 Photo-oxidation

Polymers can undergo photo-oxidative reactions when they are exposed to UV light. The mechanism describing and the different steps of photo-oxidation of polymers is shown in Figure 19[30.32]

Initiation



Propagation



Termination

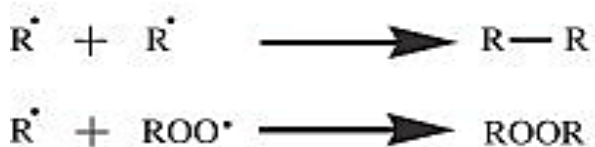


Figure 19 photo oxidation of polymer[33]

2.17.3 UV damage to polymers

Virtually all plastics products are manufactured using extrusion, injection molding, or extrusion blowing. The processing of polymers using heat and high shear into useful end products introduces impurities and reaction products that make them susceptible to photodegradation. Because of these complications, the extrapolation of research findings on UV induced degradation of pure polymer resins to compounded and processed products of the same polymer is often unreliable. Photodegradation data generated on the actual polymer formulations used in practice, processed in the conventional manner, are the most useful for assessment of damage

The many concurrent chemical processes taking place in polymers exposed to UV radiation result in several different modes of damage, each progressing at a different rate. It is usually the critical first-observed damage process that determines the useful service life of the product. For instance, discoloration, yellowing, chalking, loss of impact strength, and a reduction in tensile properties as well as a host of other chemical changes. The two critical modes of photodamage applicable to most natural and synthetic materials are yellowing discoloration and loss in mechanical integrity.[34,35]

Yellowing discoloration; Change in color is usually the first indication of weathering followed by surface flaws which eventually becomes stress centers for crack initiation. A slightly discolored part likely has still an excellent mechanical performance. The color change depends strongly on the initial color and color pigments used. Both natural biopolymer materials and synthetic polymers undergo UV-induced discoloration, usually an increase in the yellowness on exposure. And also for transparent materials it causes the loss of transparency, the haze increases and transmission reduces over time due to erosion of the top surface and causes mattening (becoming opaque) on the surface. The effect of weathering is more severe in transparent grades compared to opaque grades, as many pigments used in opaque colors (such as titanium dioxide) shield the polycarbonate from UV rays by UV absorption or reflection.[36] As an example of polymer used in building applications, mainly as glazing, is polycarbonate. When irradiated with short-wavelength UV-B or UV-C radiation, polycarbonates undergo a rearrangement reaction (referred to as a photo-Fries rearrangement). At low oxygen levels this reaction can yield yellow-colored products such as o-dihydroxy-benzophenones [37,38]. But when irradiated at longer

wavelengths (including solar visible wavelengths) in the presence of air, polycarbonates undergo oxidative reactions that result in the formation of other yellow products

The loss of strength, impact resistance, and mechanical integrity of plastics exposed to UV radiation is well known. These changes in bulk mechanical properties reflect polymer chain scission (and/or cross-linking) as a result of photodegradation. Changes in solution viscosity and the gel permeation characteristics of polymers have been used to establish molecular changes during photodegradation.[34]

Photo-chemical reactions in polymer can induce various changes in physical and optical properties of polymer such as solubility, transparency, thickness, and refractive index [39]. The photo-chemical reaction can induce larger refractive index modulation in polymer and the modulation remains after the photo-reaction, leading to the permanent change in refractive index.[40]

2.18 Importance of short wavelength

Photochemical degradation is caused by photons of light breaking chemical bonds. For each type of chemical bond there is a critical threshold wavelength of light with enough energy to cause a reaction. Light of any wavelength shorter than the threshold can break the bond, but longer wavelengths of light cannot break it-regardless of their intensity (brightness). Therefore, the short wavelength cut-off of a light source is of critical importance. For example, if a particular polymer is only sensitive to UV light below 295 nm (the solar cut-off point), it will never experience photochemical deterioration outdoors. If the same polymer is exposed to a laboratory light source that has a spectral cut-off of 280 nm, it *will* deteriorate. Although light sources that produce shorter wavelengths produce faster tests, there's a possibility of anomalous results if a tester has a wavelength cut-off too far below that of the material's end use environment.

2.18.1 Light stabilizers for plastic materials

To provide an appropriate protection against UV radiation, several stabilizing systems can be utilized in plastic materials. The most important types of light stabilizers are Ultraviolet Light Absorbers, Energy Transfer Agents or Quenchers, as well as Hindered Amine Light Stabilizers. A brief description of these different light stabilizers is given below.

2.18.1.1 UV light absorbers

Absorbers convert harmful ultraviolet radiation to harmless infrared radiation or thermal energy, which is dissipated through the polymer matrix. They can be either transparent as hydroxybenzophenone or opaque like carbon black.

2.18.1.2 Carbon black

Carbon black is one the most efficient and widespread light absorbers. Its efficiency as a UV absorber depends primarily on the primary particle size and structure. At the same loading, carbon black aggregates based on fine prime particles will present more surfaces to incident light - and hence a larger ultraviolet light absorbing efficiency than a coarser grade.

2.19 Types of Weathering

There are two basic types of weathering

- Natural
- Artificial
 - Accelerated Natural

2.19.1 Natural weathering

Outdoor exposure is performed on samples mounted on testing racks oriented under standard conditions (typically facing South in the northern hemisphere, 45° vertical inclination). In this way, the material is exposed to the full radiation spectrum from the infrared to the ultraviolet ranges. Of course radiation, but also temperature, and relative humidity levels strongly depend on the location; the seasons and can show some fluctuation from year to year. The average solar radiation levels for the different Cabot testing sites are the following:

Cabot Natural / Outdoor Facilities		
Exposure site	Climate Type	Yearly Solar
Dukinfield (UK)	Oceanic temperate	65 kLy
Grigno (I)	Mediterranean	100 kLy
Berre (F)	Mediterranean	110 kLy
Hong Kong	Tropical	120 kLy
Altona (Aus)	Tropical	135 kLy

$$1 \text{ kLy} = 1 \text{ cal/cm}^2 / 1 \text{ kLy} = 41.84 \text{ MJ/m}^2$$

Figure 20 Natural weathering solar exposure

2.19.2 Laboratory Weathering

Besides natural weathering, several test methods have been developed using artificial light sources to provide accelerated test procedures. All methods are based on the regular observation of characteristics reflecting an ageing process such as mechanical properties (elongation at break, tensile properties or impact strength) or visible characteristics, such as crack formation, chalking, changes in color or gloss.

The main testing methods for plastic material ageing are the following:

- a) Natural weathering stations
- b) Artificial accelerated weathering chambers:
 - QUV fluorescent light source
 - ATLAS Xenon lamp
 - SEPAP chamber (medium pressure mercury arcs)

2.19.3 Artificial weathering chambers

- Xenon Arc Instruments
- Fluorescent UV Devices
- Metal Halide Systems
- Carbon Arc Instruments
- Corrosion Cabinets

Because there is a need for more rapid evaluations of the resistance of materials to weathering than can be obtained by outdoor exposure tests, devices with artificial light sources are generally used to accelerate the degradation. These sources include filtered long arc xenon, fluorescent, metal halide lamps and carbon arc. Less commonly used light sources include mercury vapor and tungsten lamps. These laboratory accelerated weathering tests are sometimes, and perhaps more appropriately, referred to as artificial weathering.

The acceleration over natural weathering occurs for several reasons. Principally, the tests can run continuously at naturally occurring or higher irradiance than solar radiation, uninterrupted by the natural day/night cycle, seasonal variations, and weather conditions. Temperatures, thermal cycles, humidity, and water exposure also can be manipulated to maximum, but not unrealistic, stress levels. Specimens can be exposed to spectral energies at or beyond the limits of their intended service exposures, although caution must be exercised so as not to cause unnatural degradation mechanisms. In addition to the ability to manipulate and accelerate weathering conditions on demand, a fundamental benefit of a laboratory test is the reproducibility and repeatability over what is essentially an uncontrolled and variable phenomena, the actual weather. Research can be conducted to study the specific response of materials to various weathering factors. Each of the weathering factors can be controlled independently. Each light source has its own inherent benefits (and pitfalls) of which a weathering experimenter must be aware. Since the radiant energy received by an exposed material is considered to be most important, we will focus our attention on the quality of the light source, referring to how well each light source resembles natural sunlight and simulates other outdoor factors

a) QUV fluorescent light source

Weathering chambers have been developed to provide a QUV weathering. The QUV simulates the effect of sunlight with fluorescent ultraviolet (UV) lamps, while rain and dew are simulated by the condensation of humidity. As stated previously, the UV light only represents roughly 5%

of the sunlight but it is responsible for most of the polymer degradation. Also, materials are often tested with equipment, which simulate only the shortest wavelengths (UV). The UV-

B range includes the shortest wavelengths found in sunlight. Therefore, for many applications, it is a fast and efficient method. QUV equipment uses two main types of lamps: UVA-340 and UVB-313. Lamps have different light emission spectrum, they are both characterized by a maximum of emission in the UV range. UVA provides a reasonable match of the UV region of the solar spectrum, but this match is no longer valid for the long wavelengths (visible, IR). UVB lamps also emit UV light, but the maximum of the emission spectrum is shifted towards short wavelengths compared to the UVA lamps. The UVB-313 lamp is a widely used type of fluorescent UV lamp that provides fast test results. However, the spectrum contains short wavelengths, which are not present in the solar radiation. For customer support, Cabot typically uses UVB lamps characterized by their short wavelength spectrum in order to provide fast test results. Although these data might not always perfectly correlate with outdoor exposure results, QUV-B is very useful for preliminary or comparative testing, as well as for very durable applications. For more realistic exposure conditions, ATLAS Weathering Chambers are generally preferred.

2.20 Fluorescent UV Devices

Fluorescent UV lamps, similar in mechanical and electrical characteristics to those used for residential and commercial lighting, have been developed with specific spectral distributions. These sources are incorporated into fluorescent UV condensation devices such as the Atlas UV2000. These devices may be used in tests that vary light/dark cycles, temperature, condensing humidity, water sprays, and irradiance control. Their functional design and use is primarily governed by ISO 4892-3, *Plastics— Methods of Exposure to Laboratory Light Sources Fluorescent UV-Lamps*; ISO 11507, *Paints and Varnishes — Exposure of Coatings to Artificial Weathering . Exposure to Fluorescent UV and Water*; and ASTM G154, *Standard Practice for Operating Fluorescent Light Apparatus for UV Exposure of Nonmetallic Materials*. There are several different types of fluorescent UV lamps that have unique spectral characteristics. Fluorescent UV-B lamps (F40 and UVB-313), with a peak around 313 nm, have nearly all of their energy concentrated between 280 nm and 360 nm. A large percentage is at wavelengths shorter than what is present in natural sunlight. There is very little radiation with wavelengths longer than 360 nm. Reversals in the stability ranking of materials have often been reported between laboratory

accelerated and out-door tests when the accelerated test uses UV-B lamps. This occurs because of the large amount of short wavelength UV and the lack of long wavelength UV and visible radiation; the mechanisms of degradation may be significantly different from those of the “natural” tests. Fluorescent black lights, referred to as UV-A lamps, are available with peak emissions of 340 nm – 370 nm (e.g., UVA-340 and UVA-351). In the UVA-340 lamp, developed in 1987, the short wavelength irradiance simulates that of direct solar radiation below 325 nm



Figure 21 Atlas UV 2000

Because UV-A lamps do not emit radiation below the cut-on of natural sunlight, correlation with outdoor weathering is somewhat improved, but test times are longer than with UV-B lamps. It may be noted, however, that tests using fluorescent lamps are widely practiced. These tests are useful for relative rank comparisons between materials under specific conditions. In general, fluorescent UV devices offer a condensation cycle (during a lights-off period) to produce moisture. The test surface is exposed to a heated, saturated mixture of air and water vapor. The relative humidity inside the chamber is approximately 100% during the dark cycle. The reverse side of the panel is exposed to room air that drops the panel temperature below the dew point, causing condensation (dew) on the exposed surface. The sequence and time intervals for both the ultraviolet cycle and the condensation cycle are programmable and automatic. Likewise, temperatures can be controlled (within limits) during both the UV and condensation cycles. Though fluorescent UV light sources

are widely used in materials testing, knowledge of their limitations will serve the tester well. Until recently, the UV-B bulbs have been the most popular sources. However, their use has declined due to their poor record in accurately predicting a materials' outdoor performance. The UVA-340 source is more viable as it provides a good match for the terrestrial solar spectrum between 300 and 400 nm, but is very deficient there- after, having virtually no output in the visible and infrared. This deficiency is important because it will tend to expose materials of different colors to the same surface temperature, contrary to what they would actually experience in a full spectrum source like sunlight and xenon. As we have already seen, temperature will affect degradation rates and processes. Some users of fluorescent UV testing devices like the fact that the condensation simulates dew very closely. Others state that the temperature of this condensing water is higher than any material would see in natural conditions, resulting in unrealistic water spotting

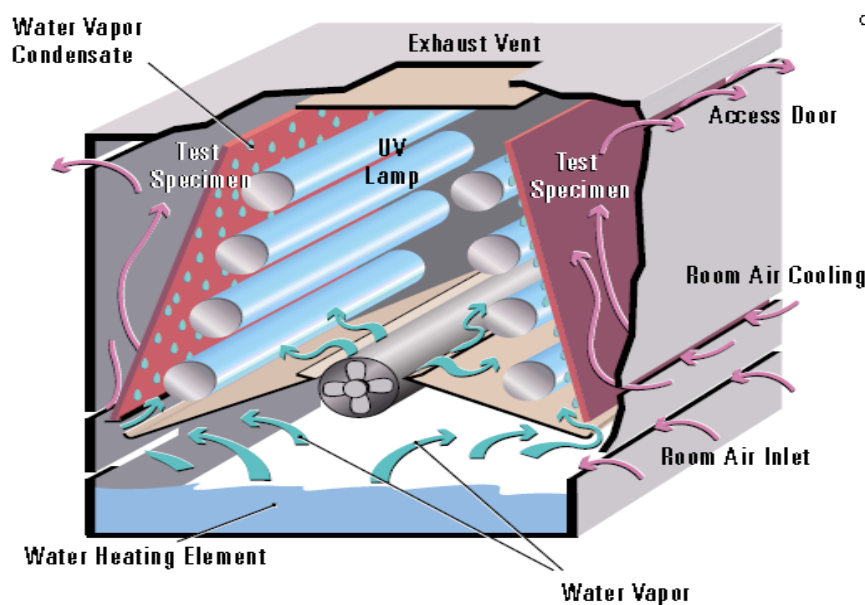


Figure 22 Atlas UV working

2.21 Tensile properties testing

Plastic optical fiber (POF) has been attracted attention because it is light, soft, flexural, impact, inexpensive, easy processing, and large numerical aperture. Widely applications of POF from communication [16-18] to decoration [19-21] under various environments have been developed and commercialized. The environmental factors (mechanical, climatic, chemical, biological and radiometric) certainly have a significant effect on the physical and chemical properties of POF, which obviously affects optical transmission performance of POF leading to the changes of lifetime of POF system [22]. The mechanical behavior of POF has been investigated. Most of these studies have focused on the attenuation induced by bends and tensile or torsion stresses [23-25]. Compared to glass fibers, POFs are made of polymers that are of lower Young's modulus, much more ductile and less stiff than silica, resulting in sufficient flexibility for installation with typical configurations.

The definitions and the equations related the tensile properties:

Stress: (σ) is the internal force per unit area. Unit is Pascal = Newton/m². According to equation :

$$\sigma = \frac{F}{A} \quad (10)$$

Tensile Strength: is the maximum stress that a material can withstand while being stretched or pulled before failing or breaking.

Strain: (ε) is a measure of how much an object is being stretched under stress..This value is the unitless value and the equation is given as:

$$\varepsilon = \frac{\Delta L}{L} \quad (11)$$

The strain is called **deformation at break** when the fracture occurred

Young's Modulus (E): is a measure of the stiffness of a material. It states how much a material will stretch as a result of a given amount of stress. Unit is Pascal = Newton/m². The equation(Hooke's Law)is given as:[41]

$$E = \frac{\sigma}{\varepsilon} \quad (12)$$

Stress-Strain Curve: the relationship between stress and strain, and all the properties that written above can be presented in stress/strain curve. An example of stress-strain curve is shown in figure(23)

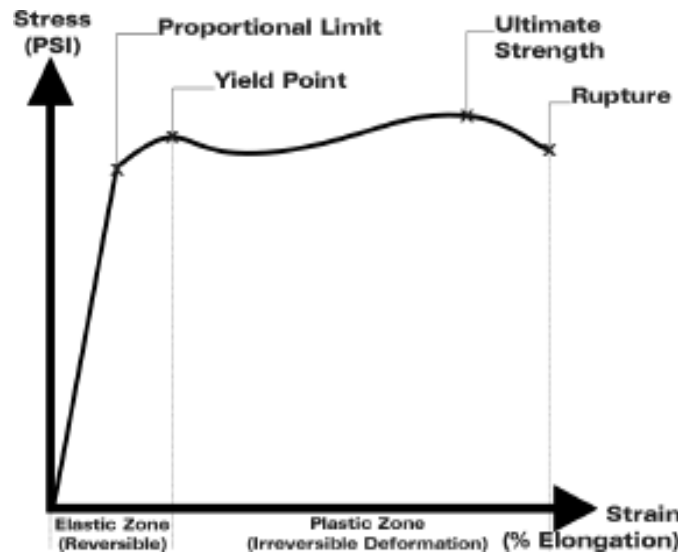


Figure 23 Stress-Strain curve

2.22 Flex fatigue of fibers

One important characteristic of polymer optical fibers is their tendency to weaken and changing side light emission capability under mechanical deformation during use.

This deformation can be simulated as repeated bending under prescribed load.

For characterization of resistance against repeated bending the flex fatigue represented by the number of repeated bending cycles till break can be used.

Flexibility of fibers is generally dependent on their diameter d and initial modulus E .

$$F_e = \frac{64}{E\pi d^4} \quad (13)$$

The flex fatigue property was carried out with self-made device. The test can be evaluated the number of samples bending cycles to failure (FC). The fiber or fabric is clamped to the upper jaw that is led by a slit (the slit is available for each fiber with the diameter from 0.2

to 3mm, and for each fabric with the maximum width of 20mm), which defines the area of bending. The upper jaw provides an adjustable pre-swing radius for samples. The pivoting jaw is driven by electric transfer PC14C54 Atas Nachod with the drive-1F SV008iC5 LS Industrial Systems. It is designed to be able to change the swing angle within 0-140° (the angle is read on a scale placed on the protective cover of the engine separating from the carrier of the sample), and a lift height of the upper jaw from the rotation is expressed by the distance from the edge of the lower jaw (such as uncontrolled free section of the sample) within 8-27 mm. The samples can be attached with suitable pretension. Measurements can be performed manually after disconnection of transmission system, which is suitable for very brittle materials. The tests are performed before setting minimum and maximum swing radius. The drive motor is set to 100, which corresponds to the swing speed of 116 per minute. The length of bend points, for example, the distance between the edge of the upper jaw and the edge of the lower jaw, is 8 mm. Each sample was tested for 50 times.

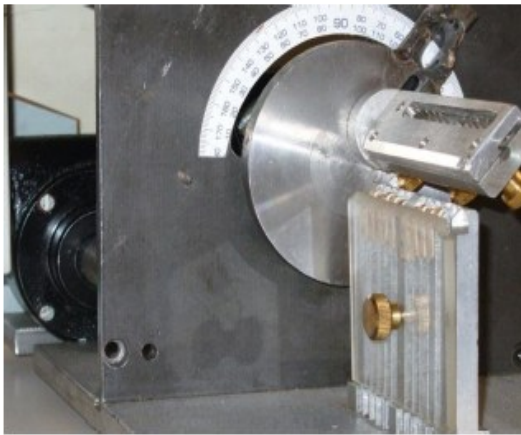


Figure 25 The prototype bending machine



Figure 24 prototype instrument

In this thesis, we used the quantile-quantile (Q-Q) plot and Weibull distribution as the exploratory data analysis methods to estimate the proper distribution of numbers of bending cycles (FC). Classical Q-Q plot is based on comparison of empirical quantile function $Q(P_i) \approx FC(i)$ with chosen theoretical quantile function $QT(P_i)$. The probability estimator $P_i = i/(n+1)$ and so-called increasing order statistics are as follows:

$$FC(1) < FC(2) < \dots < FC(N) \quad (14)$$

Weibull distribution with three parameters was used to estimate the distribution of the numbers of bending cycles to break. The function of this distribution is as follows:

$$F(FC) = 1 - \exp \left[- \left(\frac{FC-A}{B} \right)^C \right] \quad (15)$$

where A is lowest number of repeated bending cycles till break, that is shift parameter, B is scale parameter and C is shape parameter.

The suitable selection of moments was chosen and three nonlinear equations were created to calculate the three Weibull parameters. Cran used this technique for estimation of the three parameters of Weibull distribution. Parameters A, B, C can be estimated from following equations:

$$C = \frac{\ln(15)}{\ln(m_1 - m_2) - \ln(m_2 - m_4)} \quad (16)$$

$$A = \frac{m_1 m_4 - m_2^2}{m_1 + m_4 - 2 m_2} \quad (17)$$

$$B = \frac{m_1 - A}{\Gamma(1 + 1/C)} \quad (18)$$

where $\Gamma(x)$ is Gamma function. In these equations, m_r is special, so-called Weibull sample moments can be defined as:

$$m_r = \sum_{i=0}^{N-1} (1 - i/N)^r [FC_{(i+1)} - FC_{(i)}] \quad (19)$$

where $FC(0) = 0$ when $i = 0$.

Corrected Weibull 3 Q-Q plot was obtained with the linear fitting function $y = a \cdot x + b$. Here: $y = \ln[-\ln(1-p_i)]$, $x = \ln(FC(i) - A)$, $a = C$ and $b = -\ln(B) \cdot C$.

where $\Gamma(.)$ is gamma function.[43]

3 Experimental Part

3.1 Fiber composition

The fibers with trade name of GRACE and HYPOFF are used for the experiment, composition is as below.

Table 5 POF characteristics

Core/ Cladding material	PMMA/ Polyvinylidene fluoride
Diameter	from 0,25 mm to 1,5 mm
Core refractive index	1.49
Cladding refractive index	1.41
numeric aperture	0.48
maximal input angle	57.4
mass density	1190 kgm-3
weave length	400 - 900 nm
temperature of use	20 - 70°C

4 Methodology, Results and Discussion

Two kind of fibers Trademark ,GRACE and HYPOFF with different diameters were tested for Tensile properties, Light Intensity side emission and bending rigidity before and after UV-weathering at machine ATLAS UV-340. All the machines used for the experiments are explained in the review part . From results of measurements mean values and corresponding 95% confidence intervals were calculated.

For the weathering of the our samples we used the Atlas UV weathering machine, 15 hours of the Atlas UV weathering machine is equal to 1 month of outside UV weathering and to get 1 year weathered sample we put our samples for 7 days in to the machine.

4.1 Light Intensity side emission comparison

For testing the 500 cm sample size is used and 10 times measured has been done before and after UV. It is necessary to have even and smooth cross-section surface area so that after cutting the sample with suitable knife, sanding and the polishing with the diamond powder is necessary. Uneven surface will be affecting the optic properties

Surface light intensity is decreased after the weathering, fig 26-29 shows the decrease of light intensity at surface of optical fibers after the weathering for different diameter of HYPOFF fibers and figure 30 shows the comparison of surface light illumination power $P(Z)$ of different diameter of HYPOFF fibers,

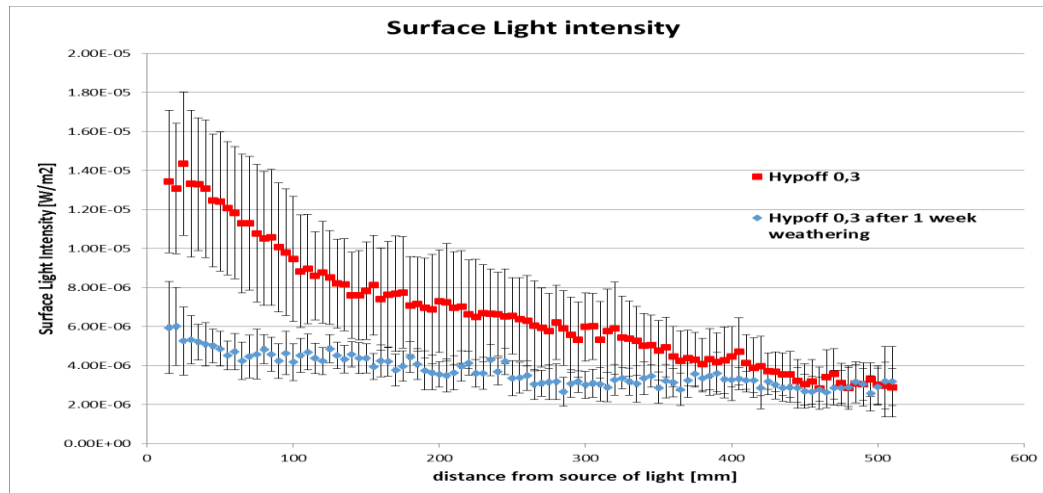


Figure 26 Comparison of light emission after weathering for HYPOFF 0.3

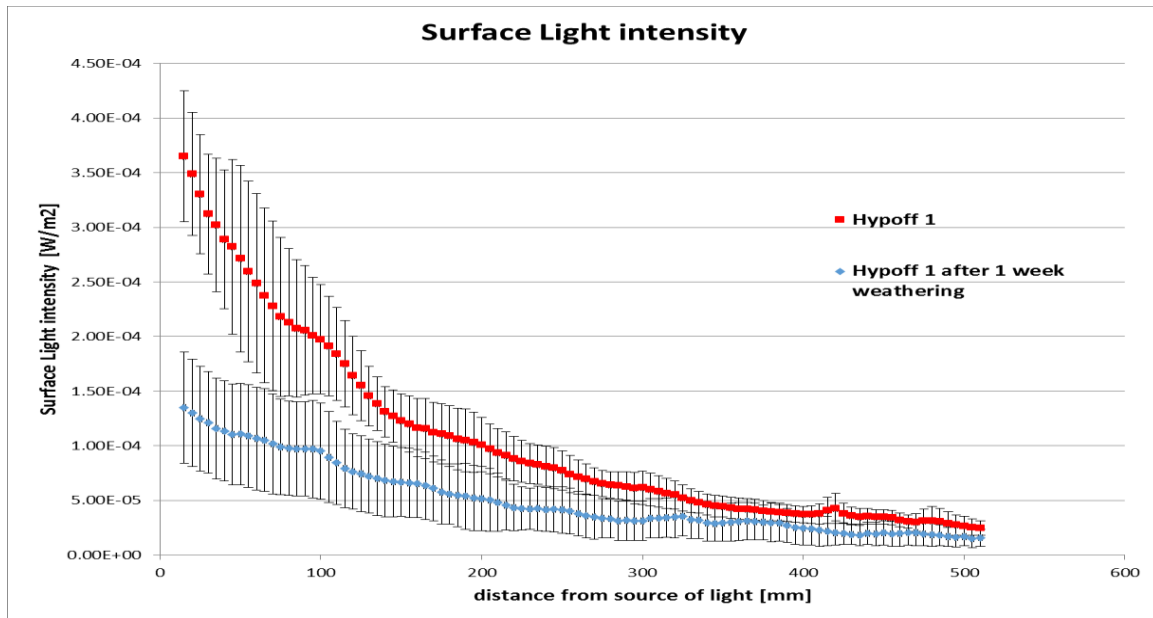


Figure 27 Comparison of light emission after weathering for HYPOFF 1

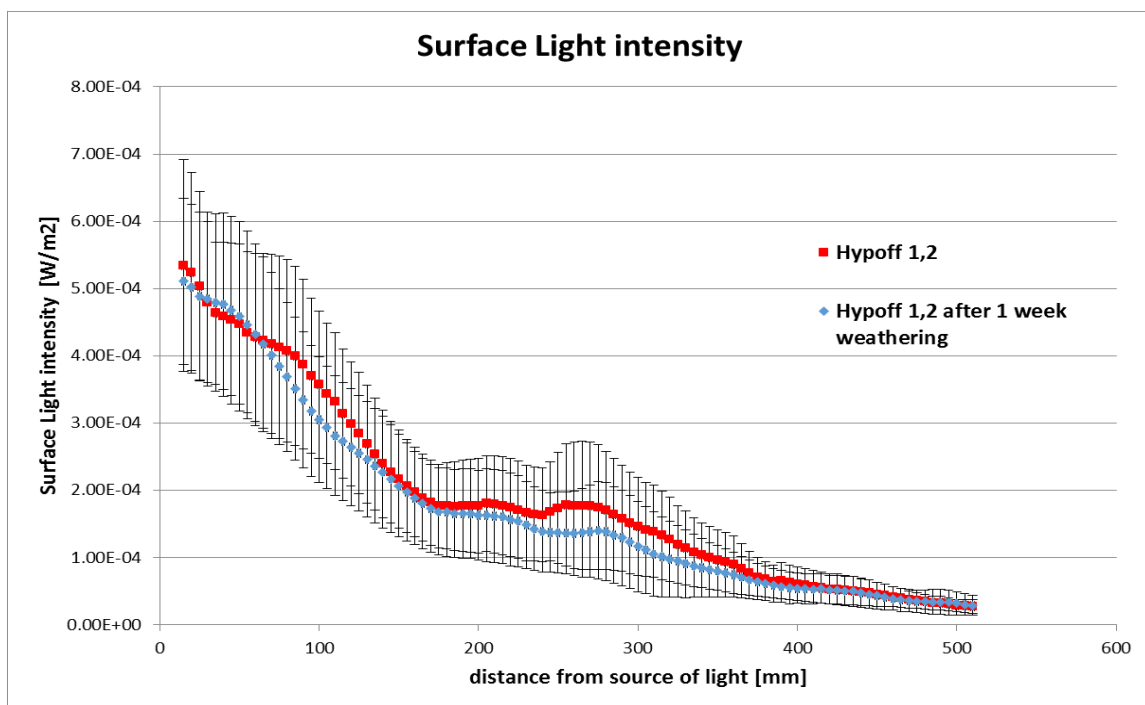


Figure 28 Comparison of light emission after weathering for HYPOFF 1.2

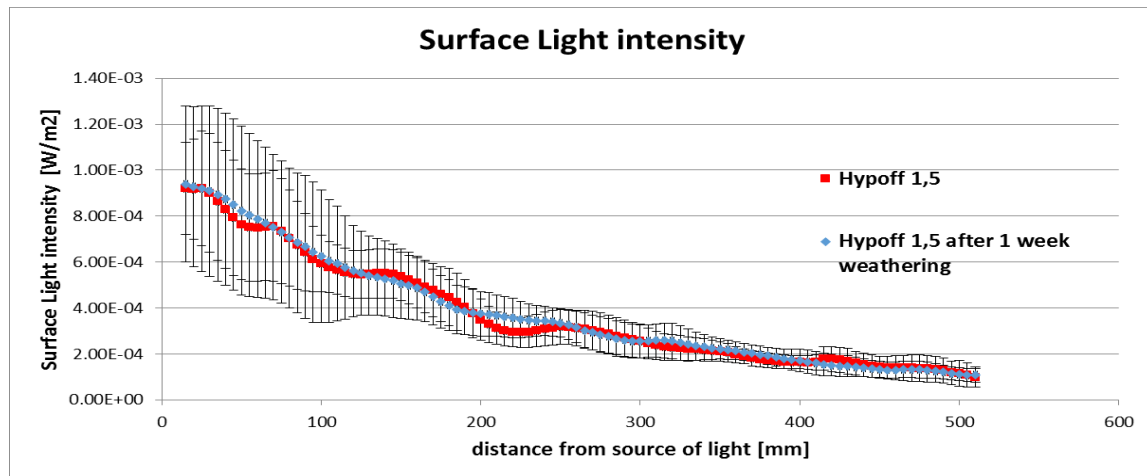


Figure 29 Comparison of light emission after weathering for HYPOFF 1.5

All fiber diameter smooth curves are included in Figure 30 which shows the surface light intensity is more with the bigger diameter whereas after weathering there is decrease in the surface light intensity of POF's

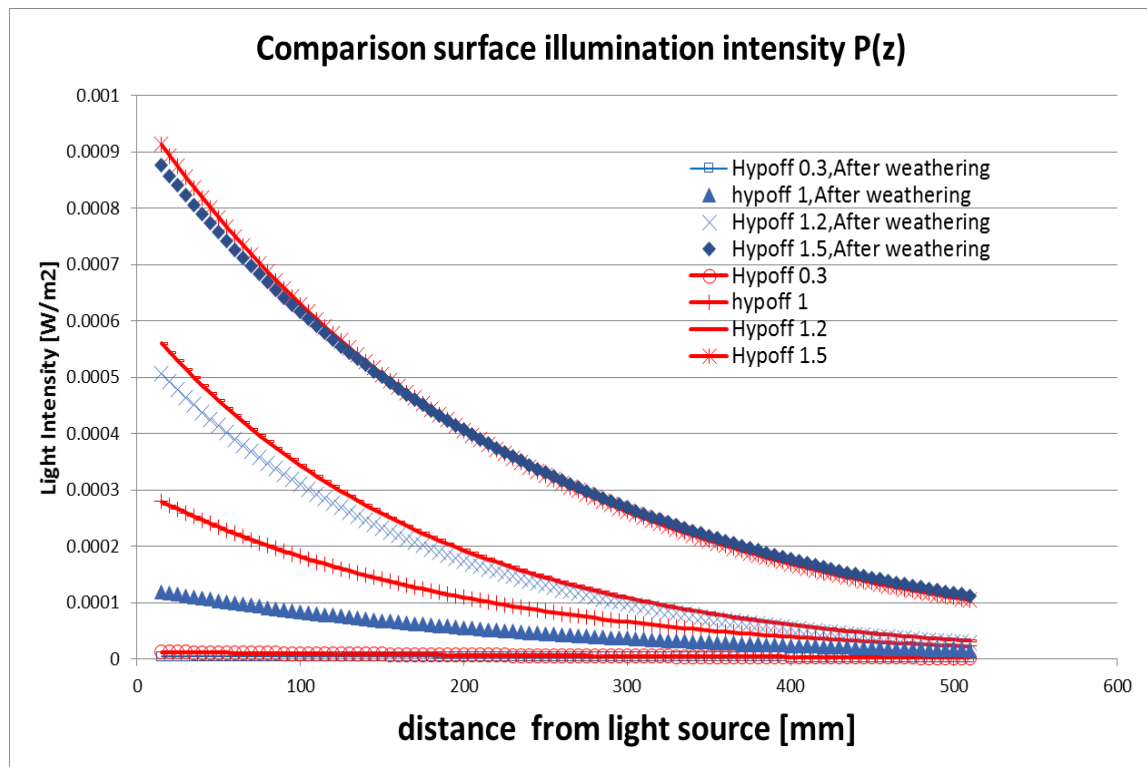


Figure 30 Comparison of surface illumination intensity $P(z)$ HYPOFF

Surface light intensity is decreased after the weathering, fig 31-34 shows the decrease of light intensity at surface of optical fibers after the weathering for different diameter of GRACE fibers and figure 35 shows the comparison of surface light illumination power $P(Z)$ of different diameter of GRACE fibers,

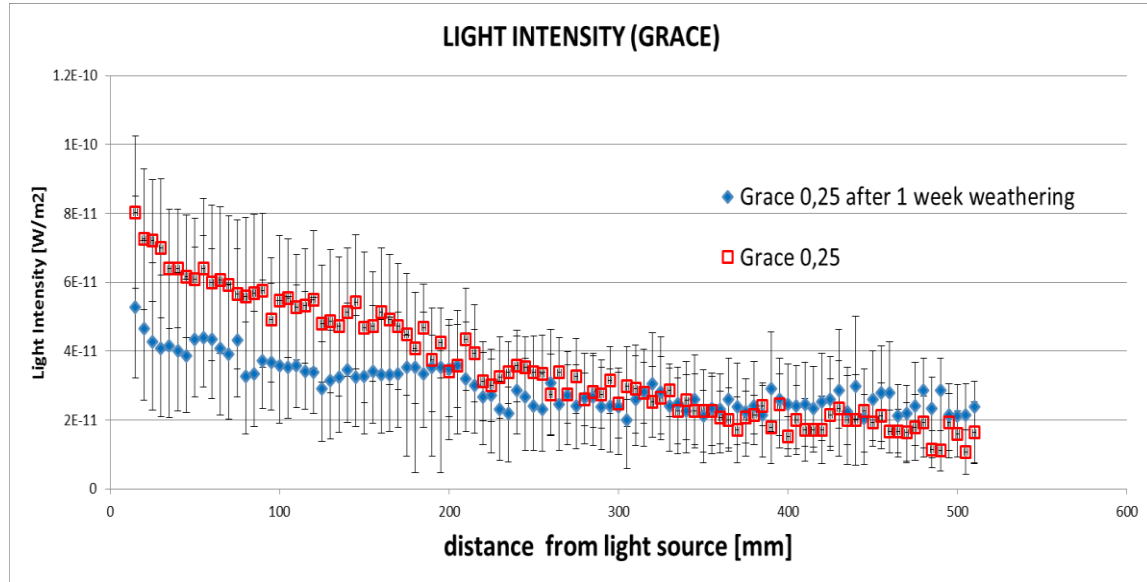


Figure 31 Comparison of light emission after weathering for GRACE 0.25

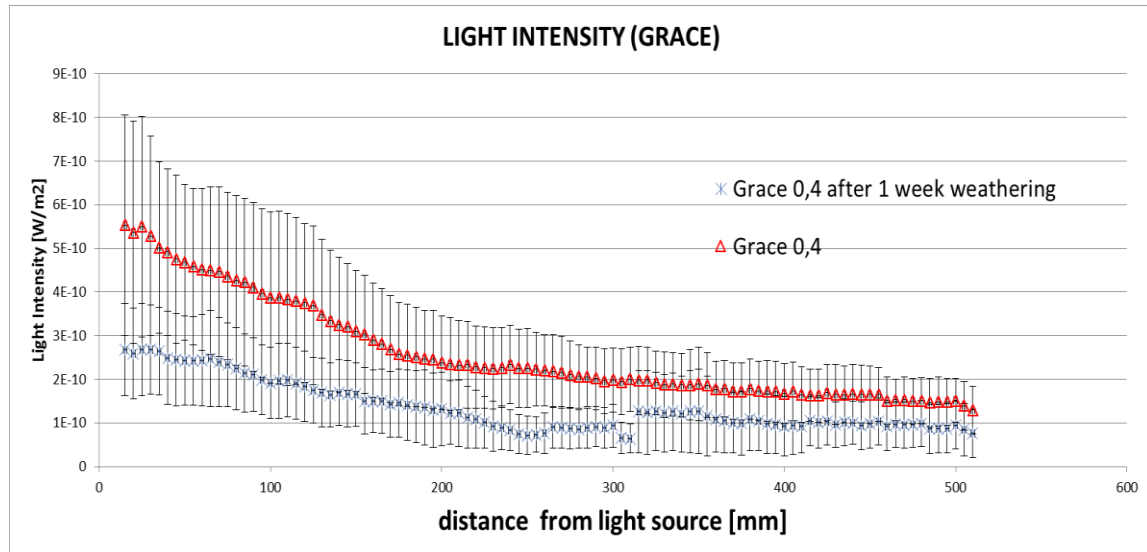


Figure 32 Comparison of light emission after weathering for GRACE 0.4

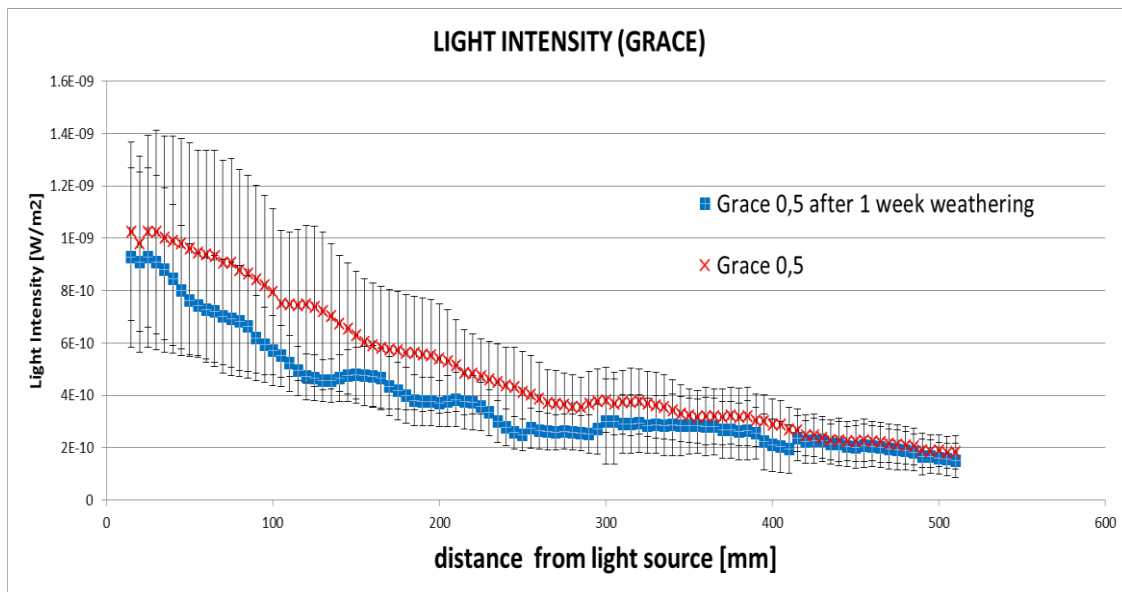


Figure 33 Comparison of light emission after weathering for GRACE 0.5

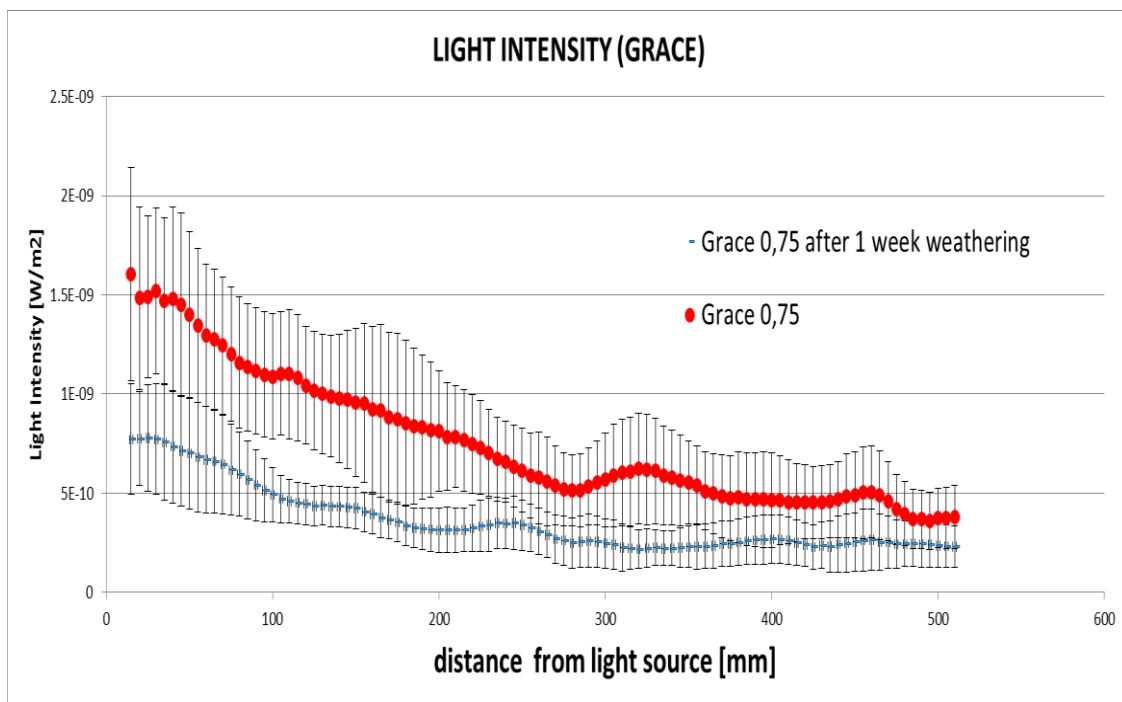


Figure 34 Comparison of light emission after weathering for GRACE 0.75

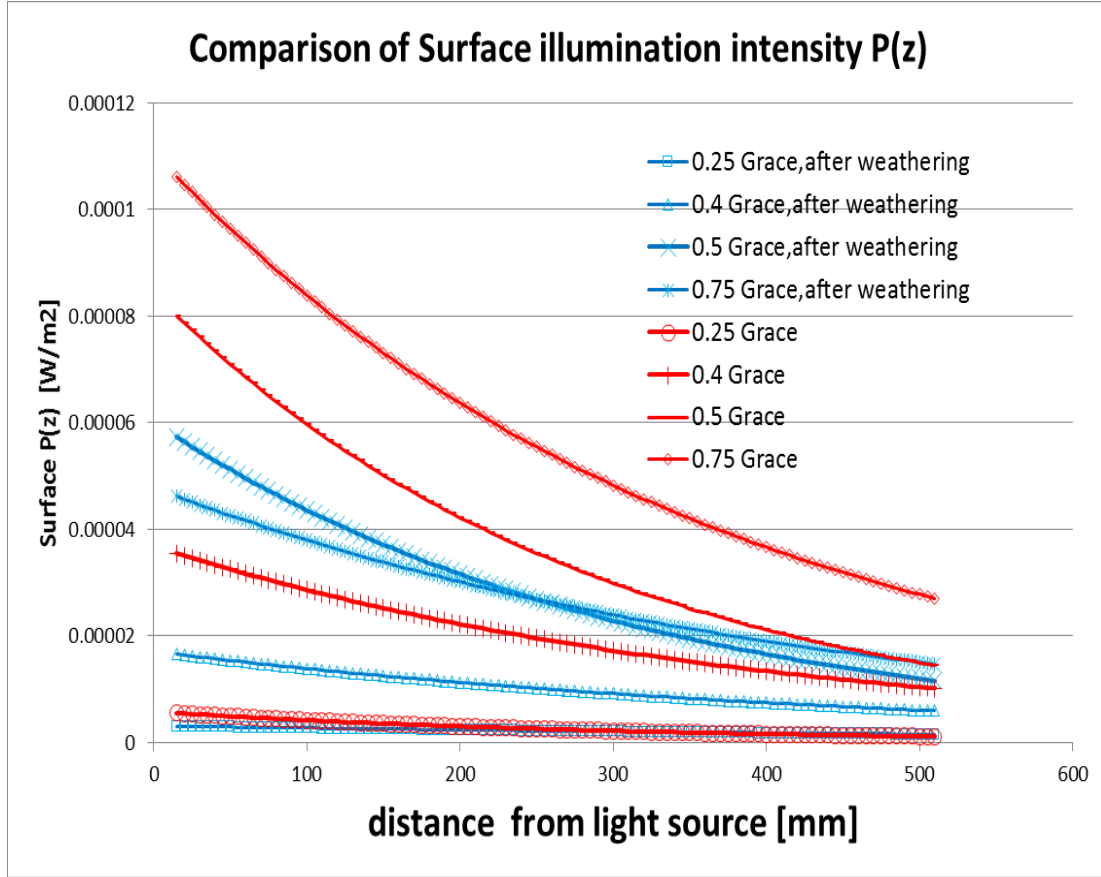


Figure 35 Comparison of Surface illumination intensity $P(z)$ GRACE

Fig 30 and 35 also shows that with the increase of fiber diameter there is more surface light illumination, so more light is allowed to reflect out of the surface in bigger diameter optical fibers as compared to smaller diameter optical fibers.

For calculating a smoothed curve, firstly the scatter plot is plotted between the Logarithmic mean values light intensity and on X-axis is distance of light source. Then a linear trend line is plotted to get equation of fitting line as .

$$Y=kx+q \quad (20)$$

Finally parameters K and q are used to calculate $P(0)$ and α

$$P(0) = 10^q \quad (21)$$

$$\alpha = -10k \quad (22)$$

The results of α are shown in Figure 36,37 for Grace and Hypoff ,before and after UV and the result of $P(0)$ is shown in Figure 38,39

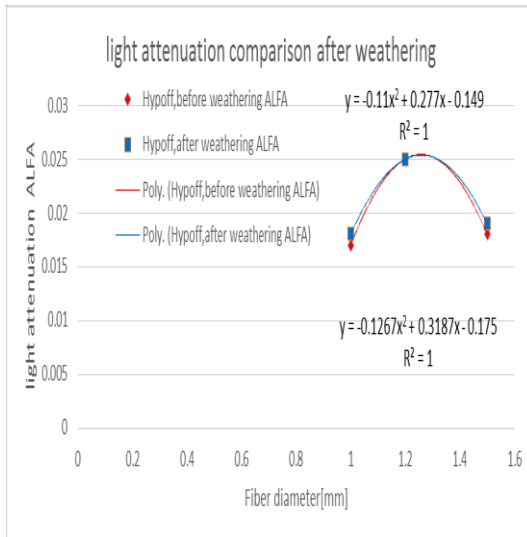


Figure 37 Light attenuation comparison, HYPOFF

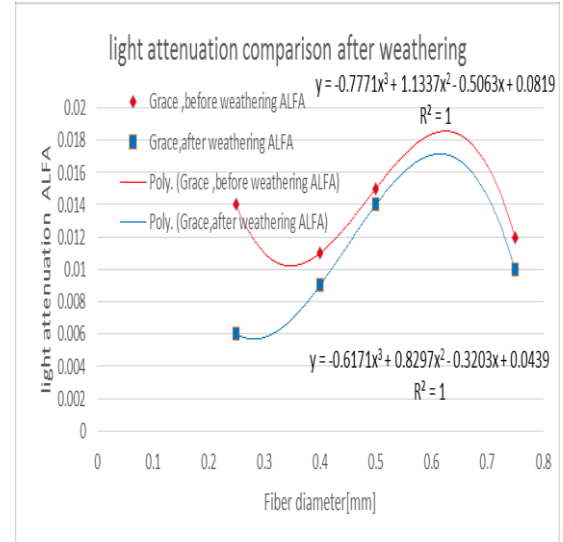


Figure 36 Light attenuation Comparison for GRACE

Fig-37 shows the light attenuation coefficient ,which has almost no impact on the HYPOFF optical fibers But Fig 36 GRACE fibers shows a decrease in light attenuation coefficient and with increase of diameter this decrease is minor.

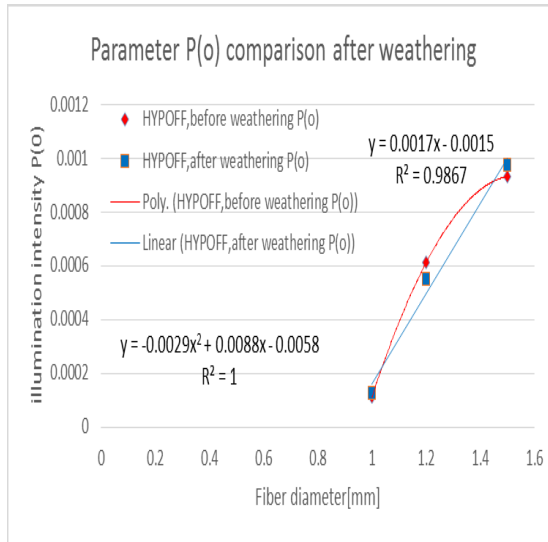


Figure 39 parameter $P(0)$ comparison for Hypoff

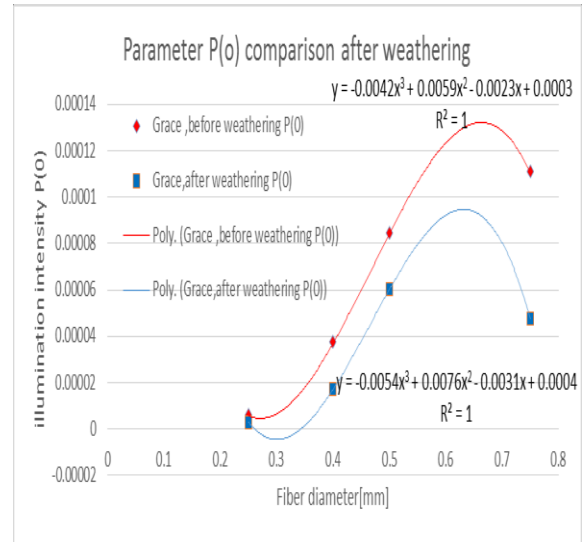


Figure 38 parameter $P(0)$ comparison for GRACE

Fig 39 shows change of parameter $P(0)$, for Hypoff fibers, with weathering , in fig-38 for the GRACE fibers shows decrease of parameter $P(0)$ after weathering.

4.2 Tensile properties

Instron-4411 tester was used for measuring mean initial modulus, mean deformation at break and tensile strength with corresponding coefficient of variation 95% confidence interval of initial modulus, deformation at break and tensile strength were calculated. The distance between two holders was 200mm, and the testing speed was 100mm/min. Each sample was tested for 50 times. Under the conditions of 23 °C and 65% RH

Testing POF's for tensile properties shows the decrease of tensile strength, initial modulus and deformation at break after weathering. Graph 43, shows a small decrease in mean initial modulus of GRACE fibers with different diameter as selected before for experiment. Whereas a higher tensile strength and deformation at break loss can be seen in fig44 &45.

Stress-Strain mean curve of GRACE fiber with diameter 0.25,0.5 and 1 mm before and after weathering comparison are shown in fig,40,41 and 42

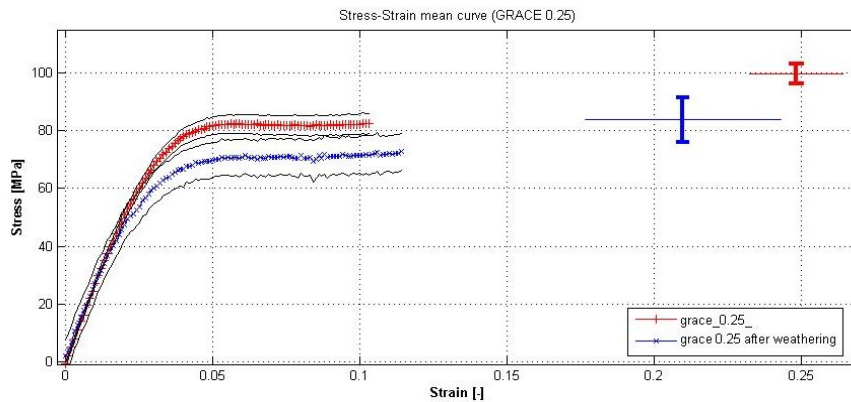


Figure 40 Stress-Strain mean curve (GRACE 0.25)

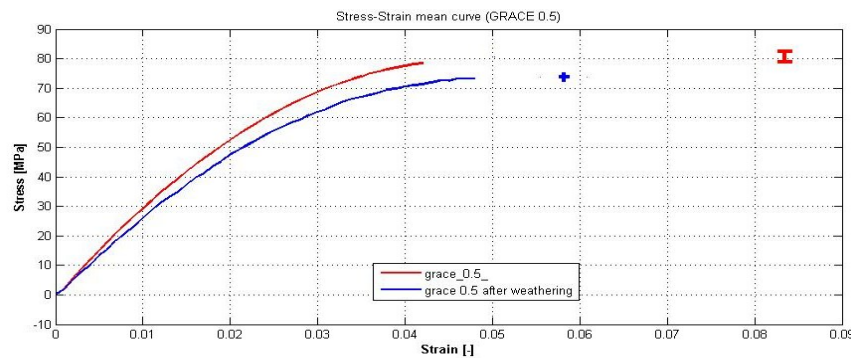


Figure 41 Stress-Strain mean curve (GRACE 0.5)

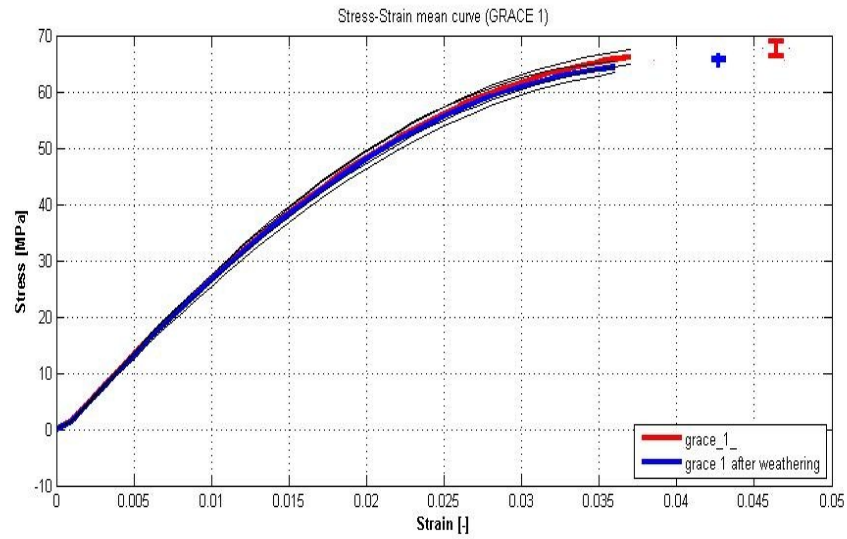


Figure 42 Stress-Strain mean curve (GRACE 1)

4.2.1 Initial Modulus

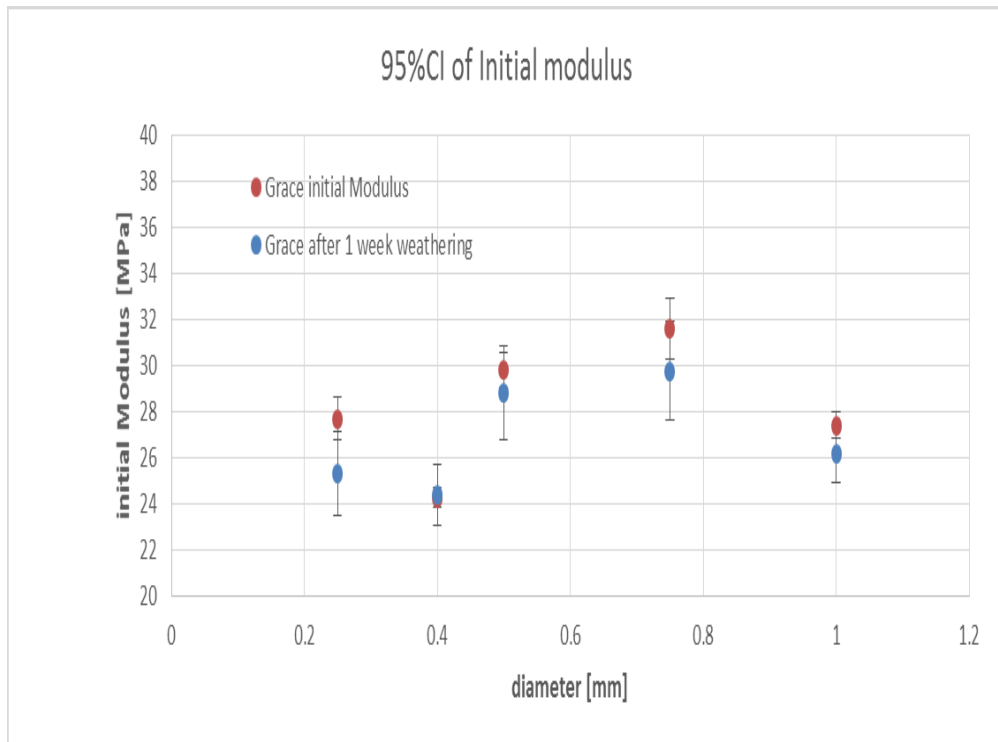


Figure 43 Mean Initial Modulus comparison (GRACE)

4.2.2 Tensile strength

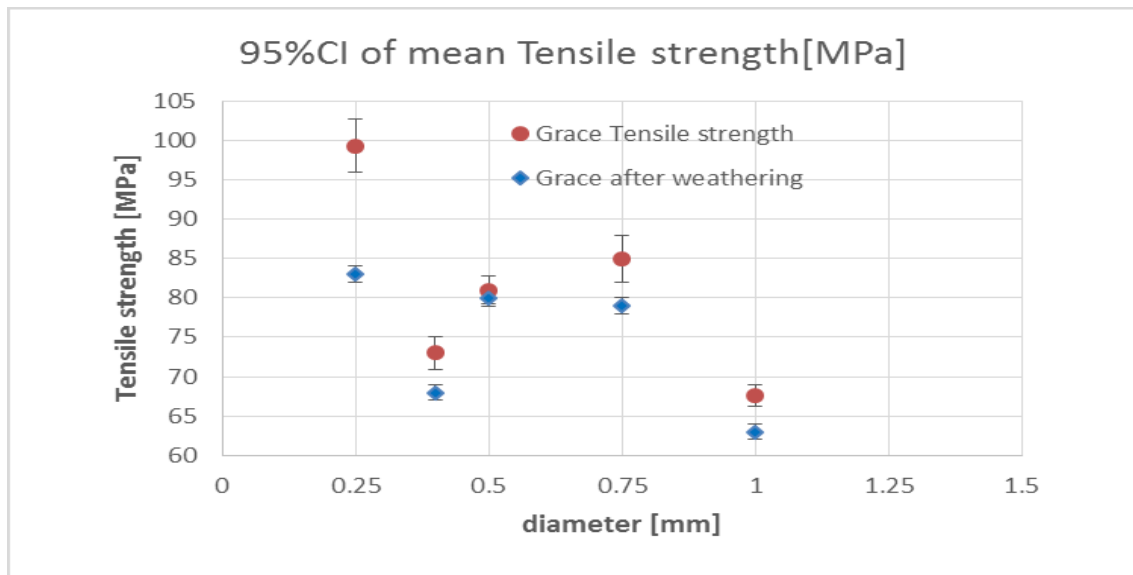


Figure 44 Mean Tensile strength comparison (GRACE)

4.2.3 Deformation at break

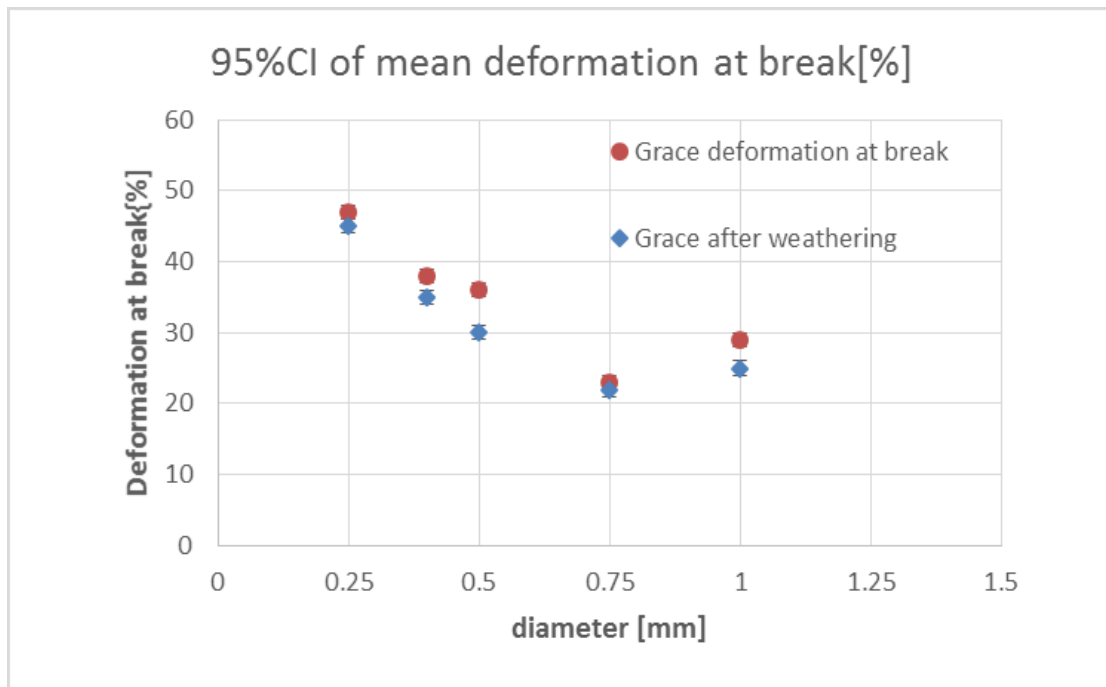


Figure 45 Mean Deformation at break comparison (GRACE)

FOR HYPOFF tensile properties, different diameter of HYPOFF POF were tested before and after weathering. Graph 48 shows a small decrease in mean initial modulus of

HYPOFF fibers with different diameter as selected before for experiment. Whereas a tensile strength and deformation at break loss can be seen in fig49 &50.

Stress-Strain mean curve of HYPOFF fiber with diameter 1.2 &1.5 mm before and after weathering comparison are shown in fig,46 &Fig 47

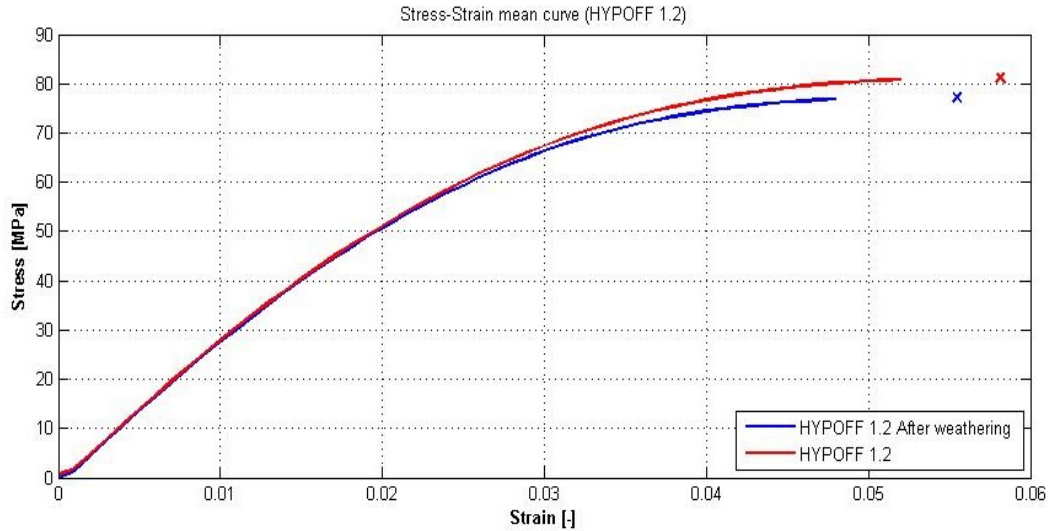


Figure 46 Stress-strain mean curve (HYPOFF 1.2)

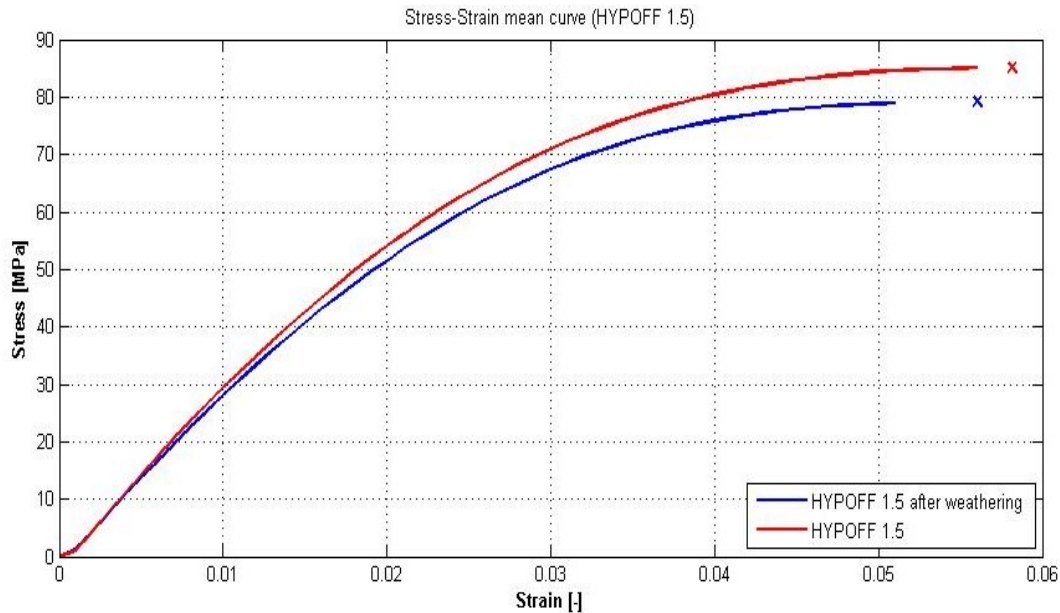


Figure 47 Stress-Strain mean curve (HYPOFF 1.5)

4.2.4 Initial Modulus HYPOFF

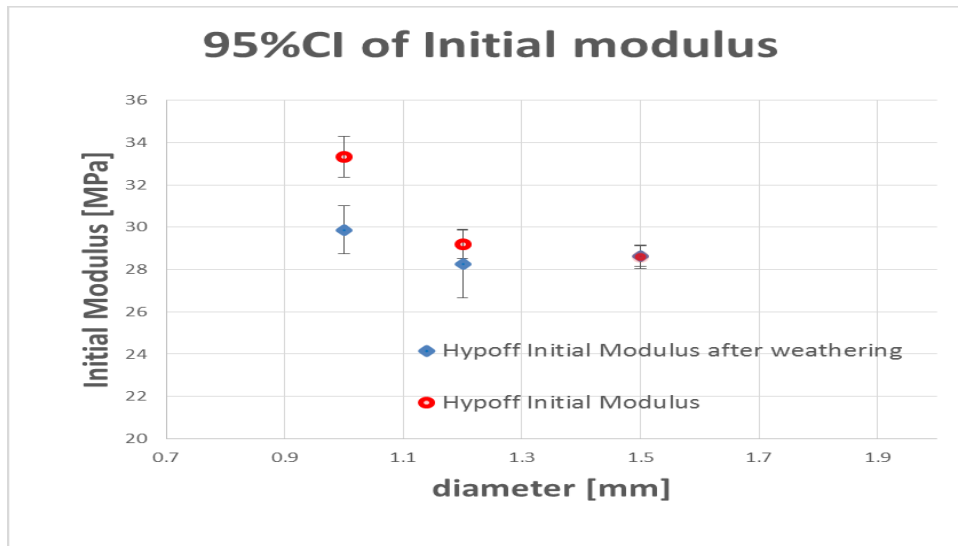


Figure 48 Mean Initial Modulus comparison (HYPOFF)

4.2.5 Deformation at Break HYPOFF

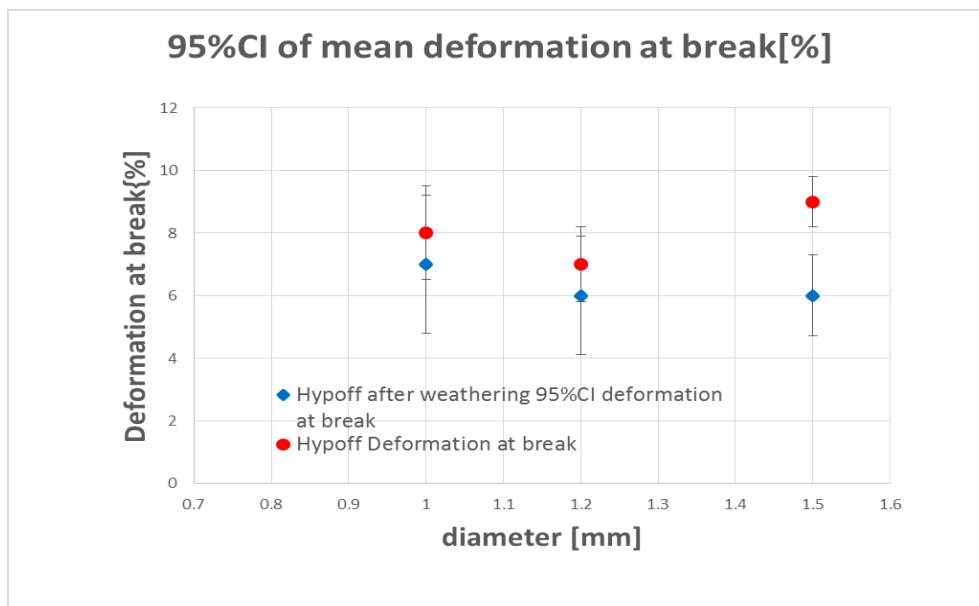


Figure 49 Mean Deformation at break (HYPOFF)

4.2.6 Tensile strength HYPOFF

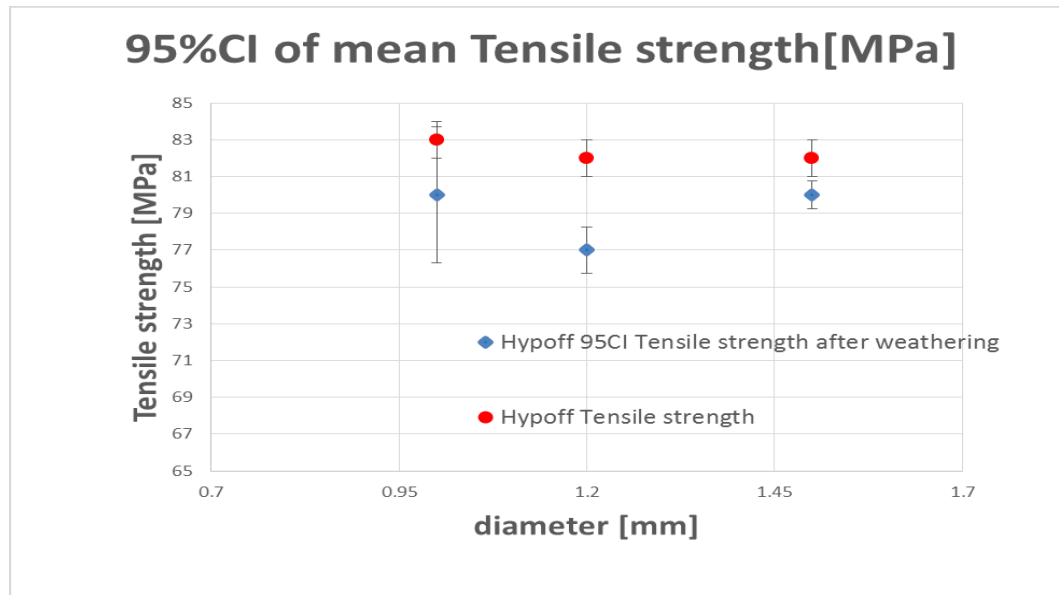


Figure 50 Mean Tensile strength comparison (HYPOFF)

4.3 Bending Rigidity

Comparatively Plastic optical fibers after weathering tend to break easily, the graph 51 shows the bending cycles to break comparison for GRACE fibers with different diameter tested before and after UV-weathering. Weibull Probability plot for Grace 0.25mm fiber before and after weathering is also shown in figure 52 and 53.

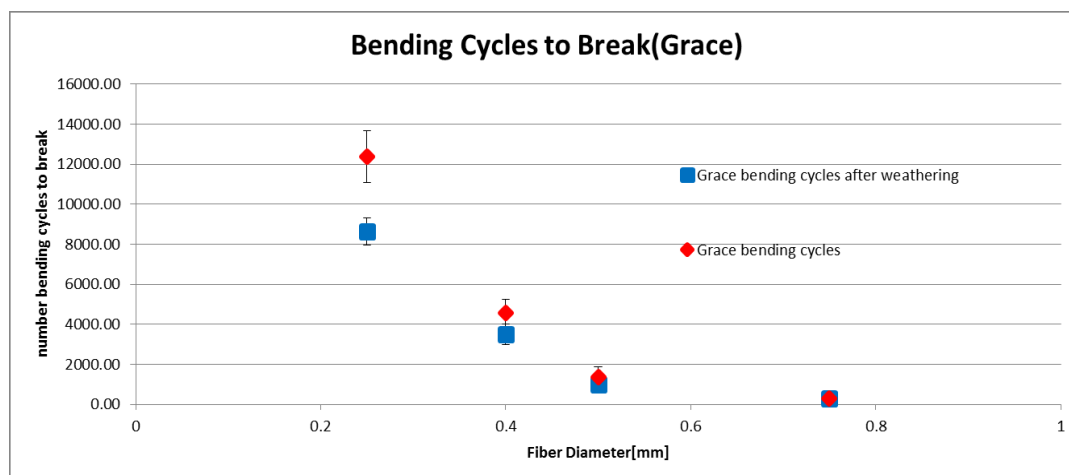


Figure 51 Bending Cycles to break GRACE

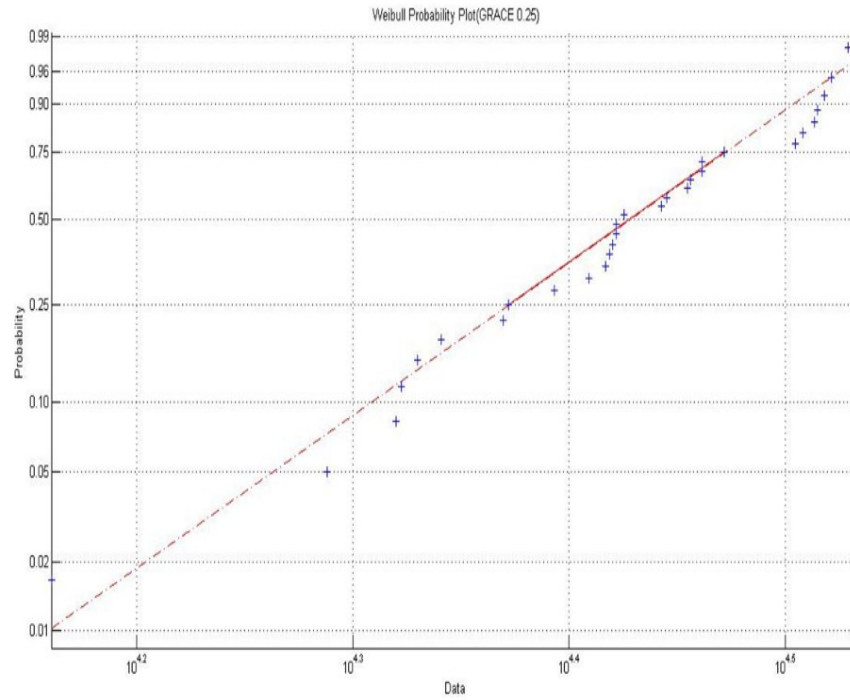


Figure 52 Weibull Probability Plot (GRACE 0.25)

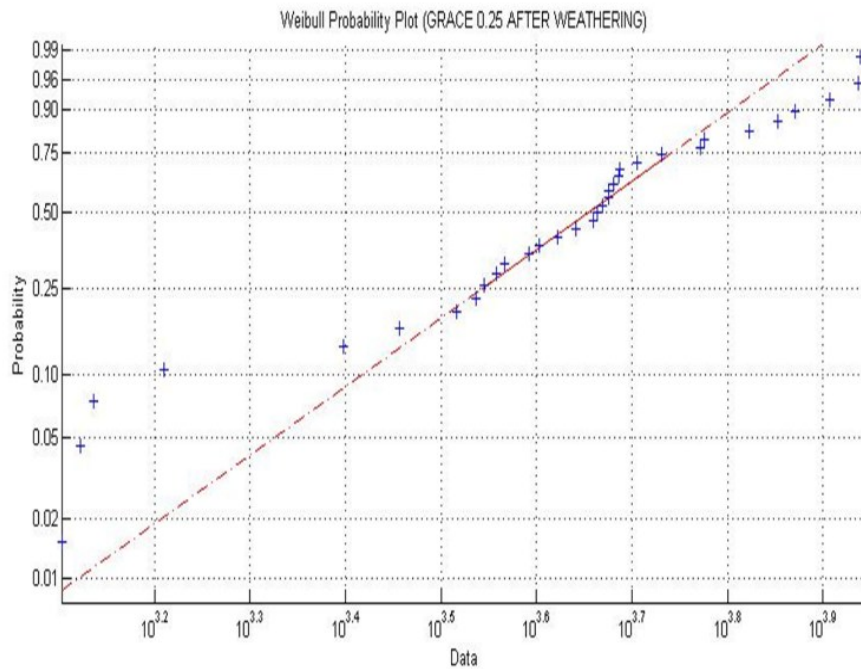


Figure 53 Weibull Probability Plot (GRACE 0.25 after weathering)

Graph 54 shows the bending cycles to break comparison for HYPOFF fibers with different diameter tested before and after UV-weathering .Weibull Probility plot for 0.3mm HYPOFF fiber before and after weathering is also shown in figure 55 and 56.

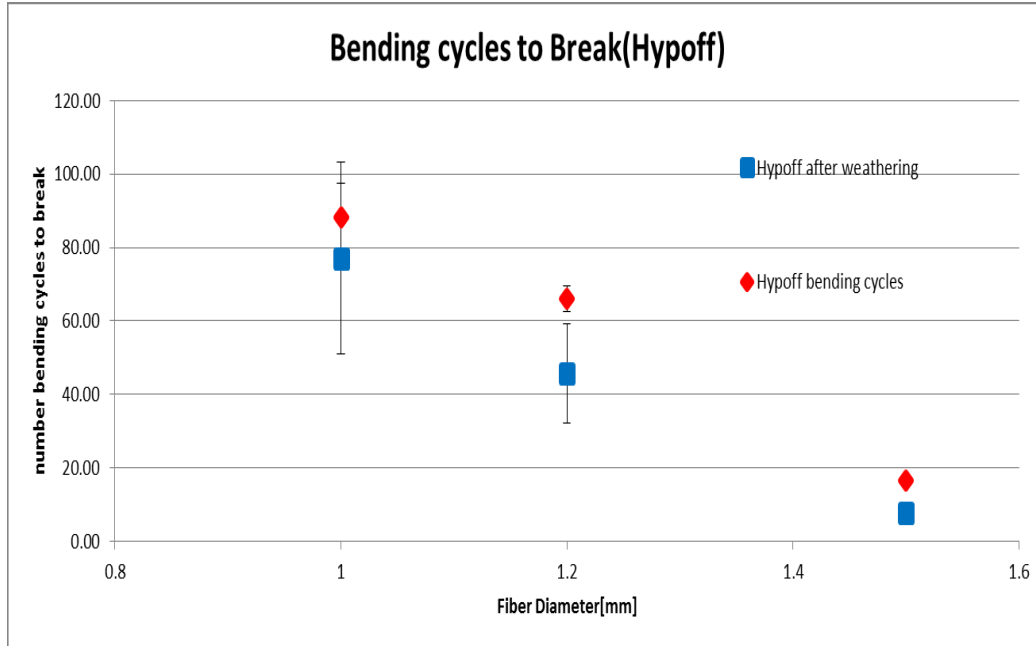


Figure 54 Bending cycles to break(HYPOFF)

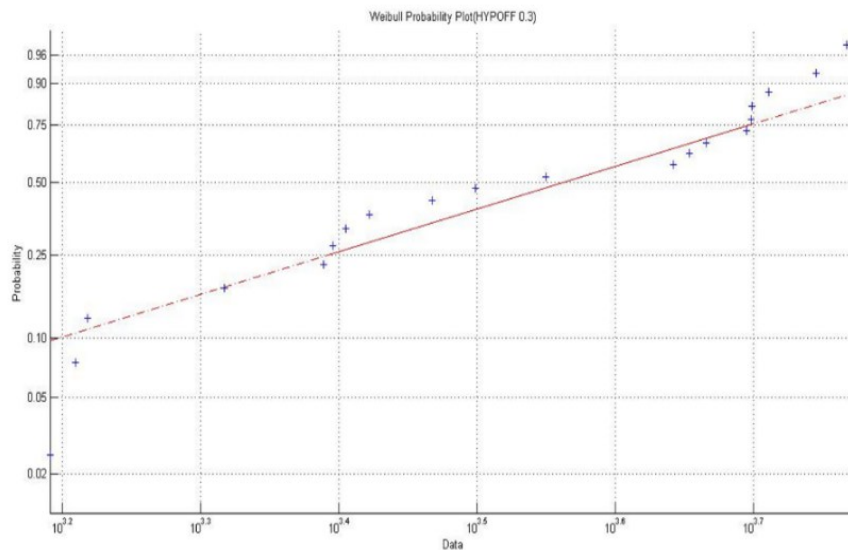


Figure 55 Weibull Probability Plot (GRACE 0.3)

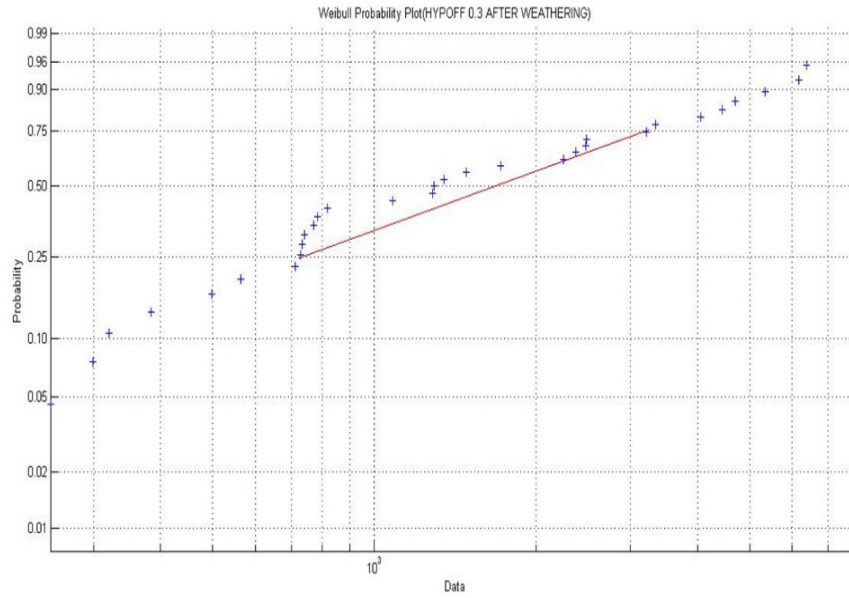


Figure 56 Weibull Probability Plot (GRACE 0.3 after weathering)

As explained in the review part the with the equations 15-19, parameters, A , B , and C of Weibull distribution were calculated as shown in table(6) below.

Table 6 Weibull Parameters

Three parameters of Weibull distribution (GRACE)						
	Before weathering			After weathering		
Diameter [mm]	Weibull shift A[Cycles]	Weibull Scale B[Cycles]	Weibull Shape C	Weibull shift A[Cycles]	Weibull Scale B[Cycles]	Weibull Shape C
0.25	834	14938	3.488	576	8050	2.59
0.5	72.5	936.2	0.6445	44.04	753	0.72
0.75	71.8	82.6	0.43	34.83	128.18	0.511
1	45.3	39.3	2.07	20.3	28.2	0.92
Three parameters of Weibull distribution (HYPOFF)						
	Before weathering			After weathering		
Diameter [mm]	Weibull shift A[Cycles]	Weibull Scale B[Cycles]	Weibull Shape C	Weibull shift A[Cycles]	Weibull Scale B[Cycles]	Weibull Shape C
1	30.42	65.04	1.79	15.5	55.34	0.82
1.2	19.1	51.71	4.09	18.91	20.76	0.68
1.5	6.11	11.89	1.99	1.95	6.2	1.27

Fig 57 and Fig 58 shows the decrease of Minimum cycles to break Parameter A of weibull distribution before and after weathering of GRACE and HYPOFF fibers.

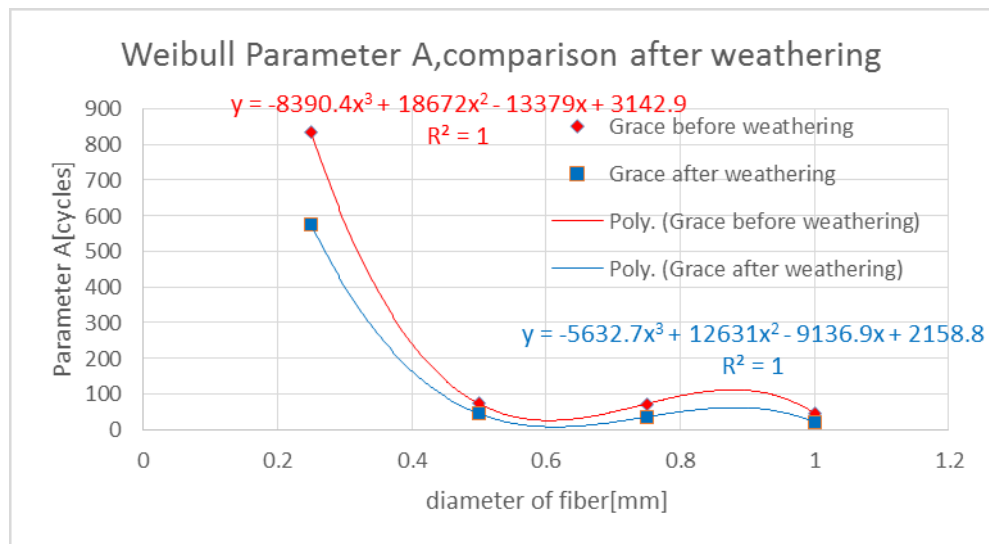


Figure 57 Weibull parameter A, GRACE

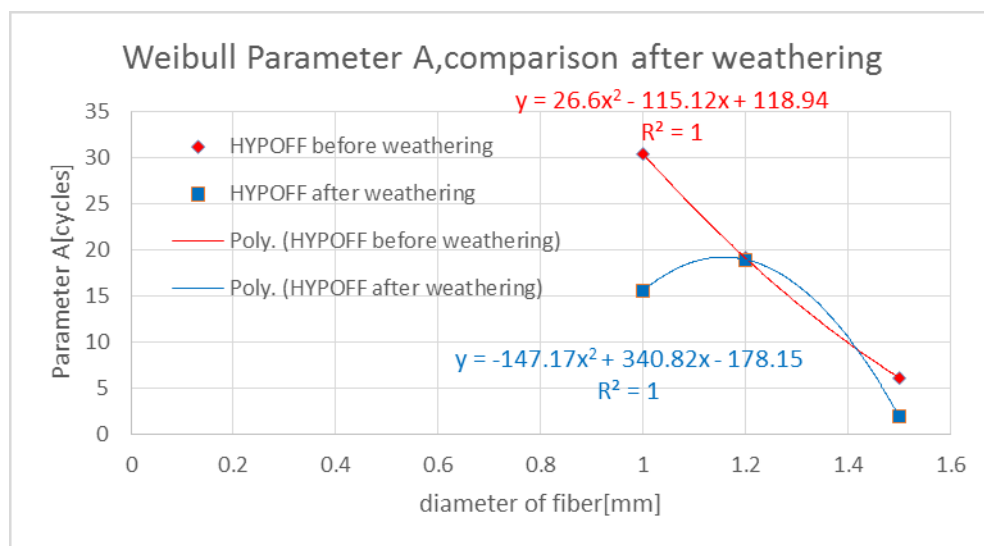


Figure 58 Weibull parameter A, HYPOFF

There is decrease of Weibull parameter A (minimum bending cycles to break) after weathering of POF. For HYPOFF the parameter A decreases with the increase of fiber diameter, but for GRACE before weathering there is a significant decrease of parameter A with increase of fiber diameter, whereas after weathering fiber diameter 1 and 1.5 shows a decrease but fiber diameter 1.2 shows a minor decrease of property parameter A.

4.4 Flexibility

Flexibility is calculated from equation 13 from initial modulus and diameter of fiber, fibers with different diameters are shown in fig59 and 60 ,Flexibility decreases with increase of diameter ,whereas after weathering there is a slight increase of flexibility as the initial modulus is decreased and difference is higher in the lower diameter fibers, as the lower diameter fiber are more impacted by UV-weathering.

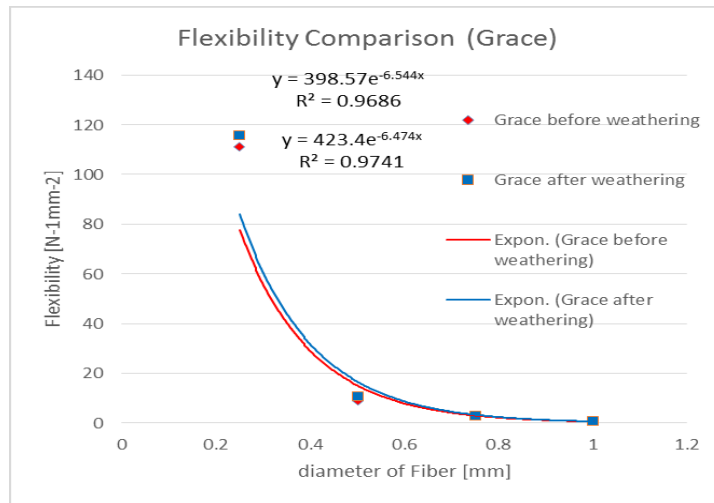


Figure 59 Flexibility comparison GRACE

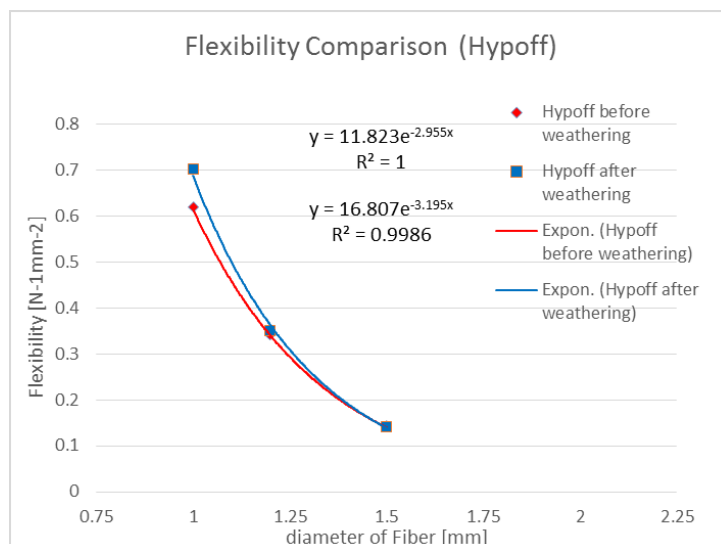


Figure 60 Flexibility comparison HYPOFF

4.4.1 SEM pictures

The samples were scanned under electron microscope for before and after weathering of optical fibers, there is minor difference in the surface quality of the optical fibers where as more difference is visible in the higher diameter, Images are shown below.

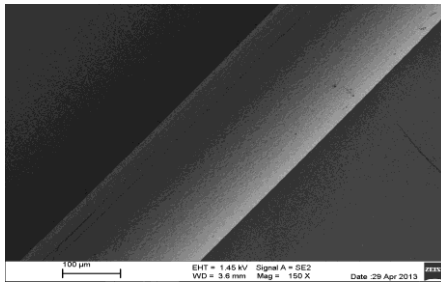


Figure 61 0.25 GRACE before weathering

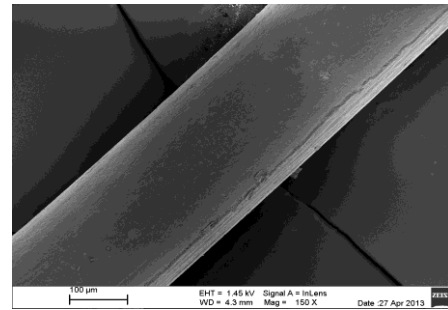


Figure 62 0.25 GRACE after weathering

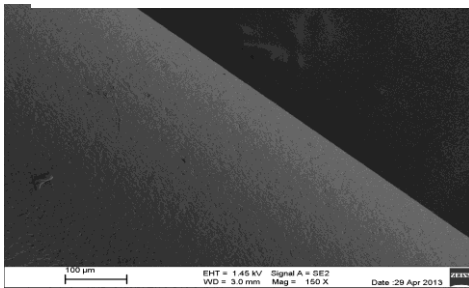


Figure 64HYPOFF 1.2 before weathering

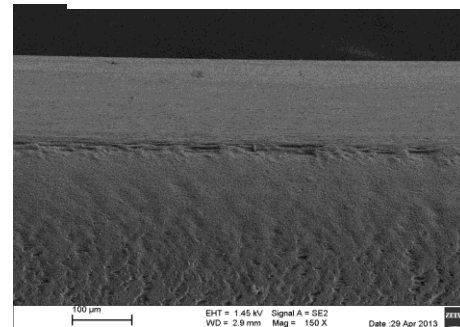


Figure 63HYPOFF 1.2 after weathering

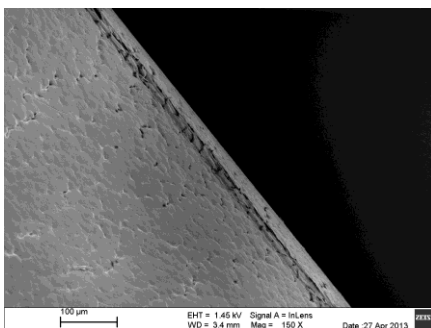


Figure 66HYPOFF 1.5 before weathering

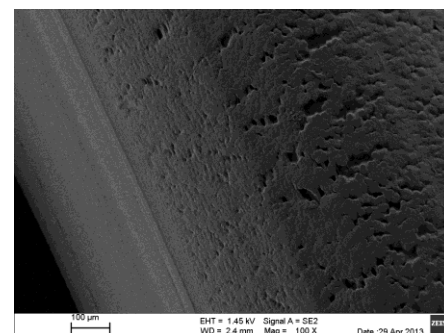


Figure 65HYPOFF 1.5 after weathering

5 Conclusions

Higher diameter fibers has higher illumination intensity but higher attenuation coefficient, lower repeated number of cycles to break and lower flexibility. It is concluded from the above research results that UV-weathering causes loss in surface light intensity in which the bigger diameter of POF's provides higher surface light intensity whereas after weathering the change in the light intensity side emission of bigger diameter fibers are almost insignificant. For application in visible safety textiles we need a good level of illuminating power and flexibility (weaving, winding). We are using POF with diameter about 1mm and the best is use fiber in straight stay or low level of waviness. After weathering POF's are easier to break due to loss in bending properties by UV-weathering and smaller diameter fibers are more impacted than the bigger diameter POF's as shown in weibull distribution parameter A, the smaller diameter shows highest flexibility and after weathering they are impacted the most. Smaller diameter POF's have more tensile strength than the bigger diameter POF's but after weathering POF's loses tensile strength, initial modulus ad deformation at break and the impact is much higher for smaller diameter optical fibers. In common Smaller diameter POF's are more impacted by UV-weathering than the higher diameter POF's as experimentally tested above for both HYPOFF and GRACE fibers with different diameter. SEM pictures show a minor difference in the surface quality of optical fibers.

5.1 Future works

- UV absorber coatings and textile covers to protect POF from weathering can be better advancement in future for the use of POF.
- Accelerated weathering with condensation can be useful for predicting the POF life time in different parts of the world.
- Accelerated weathering equivalent to 2 years or 3 years can be useful in knowing the life time of POF's .

6 References

- [1]. J. Zubia, J. Arrue, Opt. Fiber Technol. 7 (2001) 101–140. Presented at the Society of Plastics Engineers Automotive RETEC. Nov. 1987.
- [2]. Searle. N. and His. R. "UV SPD of Sunlight,'J. Optical Soc. America, Vol. 55. N0.11 1965
- [3]. Paschotta, R., Physical principles and applications of different types of Optical Fibers, , Optik & Photonik, Wiley-VCH Verlag GmbH & Co. KGaA, Weinheim, June 2008
- [4]. Omar, X. A., Brief history and overview of optical fiber technology in telecommunications,
2010.<http://haxr.org/omar/papers/PDF/Omar%20X.%20Avelar%20-%20Brief%20History%20and%20Overview%20of%20Optical%20Fiber%20Technology%20in%20Telecommunications.pdf> ,Accessed: 16 November 2011
- [5]. Lanshack, cabling and connectivity superstore, Optical fiber tutorial <http://www.lanshack.com/fiber-optic-tutorial-fiber.aspx> ,Accessed: 15 January 2012
- [6]. Appajaiah, A., Climatic stability of polymer optical fibers, University of Potsdam, Germany, 2004, p 7
- [7]. Leno, S. P., Basic Geometrical Optics, Fundamentals of Photonics, module 1.3, International society for optics and photonics, Wales <http://spie.org/x17229.xml> , Accessed: 15 January 2012
- [8]. Electrical Wholesaling, The basics of fiber optics, part 2 http://ewweb.com/mag/electric_basics_fiber_optics_2/ ,Accessed: 15 January 2012
- [9]. Zubia, J., Arrue, J., Plastic optical fibers: an introduction to their technological processes and applications, Optical fiber technology 7, 2001, p101-140
- [10]. Organic chemistry, Jonathan Clayden, Nick Greeves, Stuart Warren, Peter Wothers - Oxford University Press (2001), Chapter 52, Pages 1460-1461
- [11]. Density of glass,<http://hypertextbook.com/facts/2004/ShayeStorm.shtml> Accessed: 12 December 2011
- [12]. Meryova, B., Measurement of light intensity of optical fibers, Dana Kremenakova, 2012, p70.

- [13]. Searle. N. and His. **R.** "UV SPD of Sunlight,'J. Optical Soc. America, Vol. **55**. N0.11 1965
- [14]. Grossman, D. " Know Your Enemy: The Weather." J. Vinyl Techn.. Vol. **3**. No. 1981
- [15]. Zerlaut, G. "Accelerated Weathering & UV Measurements", ASTM STP 781, p10-24,1982
- [16]. JM Senior, MY Jamro. Optical fiber communications: principles and practice, Book. 2009.
- [17]. GP Agrawal. Fiber-optic communication systems, Book. 2011.
- [18]. K Kuriki, Y Koike, Y Okamoto. Plastic optical fiber lasers and amplifiers containing lanthanide complexes, Chemical Reviews. 2002
- [19]. SS Prasad, DA Costandino Jr, RC Heising. Fiber optics illuminators and lighting system, US patent. 2002
- [20]. DD Earl, RR Thomas. Performance of New Hybrid Solar Lighting Luminaire Design, Proceedings of the 2003 International Solar Energy. 2003.
- [21]. M Tekelioglu, BD Wood, Thermal Management of the Polymethylmethacrylate (PMMA) Core Optical Fiber for use in Hybrid Solar Lighting. 2003.
- [22]. Anilkumar Appajaiah. Climatic Stability of Polymer Optical Fibers (POF), dissertation. 2005
- [23]. Guerrero H. et al. Mechanical properties of polycarbonate optical fibers, Fiber and Integrated Optics. 1998.
- [24]. T Ishigure, M Hirai, M Sato. Graded-index plastic optical fiber with high mechanical properties enabling easy network installations. I, Journal of applied polymer. 2004.
- [25]. M Sarikaya, H Fong, N Sunderland. Biomimetic model of a sponge-spicular optical fiber-mechanical properties and structure, Journal of Materials Research. 2001.
- [26]. Meryova, B., Measurement of light intensity of optical fibers, Dana Kremenakova, 2012, p70.
- [27]. Zajkowski M. Emission of flux light in `side light' fiber optic. Proc SPIE 2002; 5125: 322-327.

- [28]. Snyder AW, Love JD. Optical Waveguide Theory 2nd ed. Chapman and Hall, London 1983
- [29]. Anthony Davis and David Sims, Weathering of Polymers, 1983
- [30]. Marjolein Diepens, Photodegradation and Stability of Bisphenol A Polycarbonate in Weathering Conditions, 2009
- [31]. A. Torikai, T. Mitsuoka, K. Fueki, Wave length sensitivity of the photo induced Reaction in polycarbonate, Journal of Polymer Science: Part A: polymer Chemistry, 1993, 31, 2785-2788
- [32]. A. Rivaton, B. Mailhot, J. Soulestin, H. Varghese, J.L. Gardette, Comparison of the photochemical and thermal degradation of bisphenol-A polycarbonate and trimethylcyclohexane-polycarbonate, Polymer Degradation and Stability, 2002
- [33]. Baljit Singh, , Nisha Sharma, Mechanistic implications of plastic degradation, Polymer Degradation and Stability, 2008
- [34]. A.L. Andradý, S.H. Hamid X. Huc, A. Torikai, Effects of increased solar ultraviolet radiation on materials, Journal of Photochemistry and Photobiology B: Biology 46 (1998) 96–103
- [35]. A. Torikai, K. Chigata, K. Fueki, Photodegradation of incombustible polymer materials, Polym. Prepr. Jpn. 42 (1993) 2045–2047.
- [36]. Sabic Innovation Plastics, Weathering -a practical approach, http://kbam.geampod.com/KBAM/Reflection/Assets/10645_2.pdf
- [37]. A. Rivaton, J. Lemaire, Photooxidation and thermooxidation of tetramethyl-bisphenol-A polycarbonate, Polym. Degradation Stability 23 (1988) 51–73.
- [38]. A.L. Andradý, K. Fueki, A. Torikai, Photodegradation of rigid PVC formulations I, Wavelength sensitivity of light induced yellowing by monochromatic light, J. Appl. Polym. Sci. 37 (1989) 935–946
- [39]. A. Reiser In Photoreactive Polymers Wiley-Interscience, New York (1989)
- [40]. M.D. Migaheda, , H.M. Zidanb, Influence of UV-irradiation on the structure and optical properties of polycarbonate films, 2004
- [41]. Engineering Basics, Simple Stress and strain
<http://engineeringbasics.net/simple-stress-and-strain/>

- [42]. Barbora Meryová, Diploma Thesis 2012, Measurement of light intensity of optical Fibers, Supervisor: doc. Dr. Ing. Dana Křemenáková, Technical University of Liberec, 2012
- [43]. Juan Huang, Dana Křemenáková, Jiří Militký “Flex Fatigue of Plastic Optical Fiber” Advanced materials research, HongKong, April, 2013,